



FATİH UNIVERSITY

The Graduate School of Sciences and Engineering

**Master of Science in
Electrical and Electronics Engineering**

**DESIGN AND MORPHOLOGICAL INVESTIGATION
OF POROUS SILICON NANOSTRUCTURES IN P-
TYPE SILICON BASED ON NOVEL COMPARISON
BETWEEN TWO ELECTROCHEMICAL CELLS**

by

Zainab ABDULJABBAR YASEEN

January 2016

**M.S.
2016**



**DESIGN AND MORPHOLOGICAL INVESTIGATION OF POROUS
SILICON NANOSTRUCTURES IN P-TYPE SILICON BASED ON
NOVEL COMPARISON BETWEEN TWO ELECTROCHEMICAL
CELLS**

by

Zainab ABDULJABBAR YASEEN

A thesis submitted to

the Graduate School of Sciences and Engineering

of

Fatih University

in partial fulfillment of the requirements for the degree of

Master of Science

in

Electrical and Electronics Engineering

January 2016
Istanbul, Turkey

APPROVAL PAGE

This is to certify that I have read this thesis written by Zainab ABDULJABBAR YASEEN and that in my opinion it is fully adequate, in scope and quality, as a thesis for the degree of Master of Science in Electrical and Electronics Engineering.

Asst. Prof. Hüseyin SAĞKOL
Thesis Supervisor

Asst. Prof. Dr. Yakup BAKIŞ
Co-Supervisor

I certify that this thesis satisfies all the requirements as a thesis for the degree of Master of Science in Electrical and Electronics Engineering.

Prof. Onur TOKER
Head of Department

Examining Committee Members

Asst. Prof. Hüseyin SAĞKOL.

Asst. Prof. Yakup BAKIŞ

Assoc. Prof. Erdal KORKMAZ

Asst. Prof. Lokman ERZEN

Asst. Prof. Ömer IŞIK

It is approved that this thesis has been written in compliance with the formatting rules laid down by the Graduate School of Sciences and Engineering.

Prof. Nurullah ARSLAN
Director

January 2016

DESIGN AND MORPHOLOGICAL INVESTIGATION OF POROUS SILICON NANOSTRUCTURES IN P-TYPE SILICON BASED ON NOVEL COMPARISON BETWEEN TWO ELECTROCHEMICAL CELLS

Zainab ABDULJABBAR YASEEN

M.S. Thesis – Electrical and Electronics Engineering
January 2016

Thesis Supervisor: Asst. Prof. Hüseyin SAĞKOL

Co-Supervisor: Asst. Prof. Yakup BAKIŞ

ABSTRACT

A single tank electrochemical cell design has been successfully fabricated and compared with the standard cell (double tank cell). The systematic comparison include two main parameter ; the influence of anodization time with the electrochemical cell design, the influence of variable anodization electrolytes with the electrochemical cell design on the fabrication process of porous silicon nanostructures in p-type silicon. Morphology and pore formation of porous silicon layers were characterized by Atomic Force Microscopy (AFM) and current-voltage (I-V) measurement, photoluminescence emission by ultraviolet-lamp (254-366) nm. Three types of pores; mesopores, mesopore fill of mesopores, and macropore fill of mesopores have been obtained from designed single tank cell with (10,30 and 60) min. of anodization time ; whilst for double tank cell has been obtained with 60 min. of anodization time Single tank cell has also been differentiated from double tank cell in showing stable red-orange ultraviolet photoluminescence emission with an improvement in current–voltage measurement

Keywords: Electrochemical Cells Design, Porous Silicon Nanostructure (PSN), Atomic Force Microscopy (AFM), Ultraviolet Emission (UV)

TASARIM VE İKİ ELEKTROKİMYASAL HÜCRELER ARASINDA YENİ GÖRE DAYALI P TİPİ SİLİKON GÖZENEKLİ SİLİKON NANOYAPILARIN MORFOLOJİK İNCELENMESİ

Zainab ABDULJABBAR YASEEN

Yüksek Lisans Tezi – Elektrik ve Elektronik Mühendisliği
Ocak 2016

Tez Danışmanı: Asst. Prof. Hüseyin SAĞKOL

Eş Danışman: Asst. Prof. Yakup BAKIŞ

ÖZ

Tek bir tankı elektrokimyasal hücre tasarımı başarıyla imal ve standart hücresi (çift tank hücresi) ile karşılaştırılmıştır. Sistematik karşılaştırma, iki ana parametre arasında; elektrokimyasal hücre tasarımı ile anotlama zaman etkisi, değişken anodizasyon etkisi p-tipi silikon gözenekli silikon nano fabrikasyon sürecine elektrokimyasal hücre tasarımı ile elektrolit. Gözenekli silikon tabakalarının Morfoloji ve gözenek oluşumu Atomik Kuvvet Mikroskobu (AFM) ve akım-gerilim (IV) ölçümü, ultraviyole lamba (254-366) nm fotoluminesans emisyonu ile karakterize edildi. Gözeneklerin üç tip; mesopores gözenekli, mesopores gözenekli dolgu ve dolgu makrogözenekler (10,30 ve 60) min ile tasarlanmış tek tankı hücreden elde edilmiştir. Anodizasyon zaman; çift tank hücre için iken 60 dakika ile elde edilmiştir. Anodizasyon zaman Tek tankı hücre ayrıca akım-gerilim ölçümünde bir iyileşme ile stabil kırmızı-turuncu ultraviyole fotoluminesans emisyonu gösteren çift tank hücresinden ayırt edilmiştir.

Anahtar Kelimeler: Elektrokimyasal Hücreler Tasarım , Gözenekli Silikon Nanoyapı (PSN) , Atomik Kuvvet Mikroskobu (AFM) , Ultraviyole Emisyon (UV)

To my family

ACKNOWLEDGEMENT

I would like to express my thanks and gratitude to my supervisors Assist. Prof. Dr. Hüseyin SAĞKOL and Asst. Prof. Yakup BAKIŞ for their help, support, understanding and patience in completing my thesis.

I would like to express my thanks to the head of department Prof. Dr. Onur TOKER for his guidance in the beginning of my master thesis program.

I would like to thank Fatih university, The Graduate Institute of Sciences and Engineering for accepting me through its graduate program which has given me an opportunity to acquire erudition and scientific research.

I would like to thank my parents, who supported me financially and morally through this study and special thanks goes to my sister Dr.Ghadah A.Yiseen for all her unremittingly precious support and my little sister Sarah for her indispensable patience with me

TABLE OF CONTENTS

ABSTRACT.....	iii
ÖZ.....	iv
DEDICATION.....	v
ACKNOWLEDGMENT.....	vi
TABLE OF CONTENTS.....	vii
LIST OF TABLES.....	ix
LIST OF FIGURES.....	xi
LIST OF SYMBOLS AND ABBREVIATIONS.....	xiii
CHAPTER 1 INTRODUCTION AND OBJECTIVE.....	1
CHAPTER 2 FUNDAMENTALS OF POROUS SILICON FORMATION PROCESS.....	5
2.1 Electrochemical Etching of Porous Silicon.....	5
2.1.1 Pore morphology.....	8
2.1.2 Anodization Parameters.....	9
2.1.2.1 Electrolyte.....	10
2.1.2.2 Potential.....	10
2.1.2.3 Electrochemical cells.....	10
2.1.2.4 Anodization time.....	13
2.2 Electrochemical Etching of Porous Silicon.....	13
2.2.1 Pure Quantum Confinement.....	15
2.2.2 Involvement of Surface States and Defect Centers.....	15
2.3 LITERATURE REVIEW.....	17
2.3.1 Cell Design.....	17
2.3.2 Fabrication of Porous Silicon Nanostructures.....	18
CHAPTER 3 DESIGN, FABRICATION AND CHARACTERIZATION OF POROUS SILICON NANOSTRUCTURE (PSN).....	25
3.1 The Chemicals.....	25
3.2 Materials and Construction.....	25
3.2.1 Double Tank Cell.....	25
3.2.2 Single Tank Cell.....	27
3.3 Power Supply.....	28
3.4 Preparing a Silicon wafer.....	29
3.5 Electrolyte.....	29
3.6 The Electrochemical Cells.....	29
3.6.1 Double tank electrochemical cell.....	29

3.6.2 Single tank electrochemical cell.....	30
3.6.3 Double tank electrochemical cell	30
3.6.4 Single tank electrochemical cell.....	30
3.7 Characterization of Porous Silicon Nanostructures.	31
3.7.1 CAMAG Ultraviolet LAMP (254-366) nm	31
3.7.2 Atomic force Microscopy (AFM).....	32
3.7.2 Current Volatge characteristic.....	33
CHAPTER 4 DISCUSSION OF THE CHARACTERIZATION RESULTS	35
4.1 Atomic Force Microscopy (AFM).....	35
4.2 Ultraviolet Photoluminescence Emission of PS Layer.....	44
4.3 I–V Characteristic.....	49
CHAPTER 5 CONCLUSIONS	53
REFERENCES	54

LIST OF TABLES

TABLE

2.1	Porous Si luminescence bands.....	16
4.1	The images of PS samples under white light and UV (254-366) nm. With anodization electrolyte of HF: EtOH at ratio (1:1) in volume, With three anodization time for designed single tank.....	44
4.2	The images of PS samples under white light and UV (254-366) nm. with anodization electrolyte of HF: EtOH at ratio (1:1) in volume , With three anodization time for double tank cell.....	45
4.3	Shows the images of PS samples prepared by using designed single tank cell, under white light and UV (254-366) nm., with three alcoholic anodization electrolytes of: HF: MeOH, HF:EtOH,HF:PrOH , at ratio (1:1) in volume etched at 60 min.....	46
4.4	Shows the images of PS samples prepared by using designed single tank cell and double tank cell, under white light and UV (254-366) nm., with HF:MeOH anodization electrolyte at ration (1:1) in volume etched at 60 min.....	47
4.5	Shows the images of PS samples prepared by using designed single tank cell and double tank cell, under white light and UV (254-366) nm., with HF:EtOH anodization electrolyte at ratio (1:1) in volume etched at 60 min.....	48
4.6	Shows the images of PS samples prepared by using designed single tank cell and double tank cell, under white light and UV (254-366) nm., with HF:PrOH anodization electrolyte at ratio (1:1) in volume etched at 60 min.....	48

LIST OF FIGURES

FIGURE

1.1	Change of properties from bulk to Porous silicon.....	2
2.1	Schematic diagram showing Electrochemical cell used for the preparation of porous silicon in HF-based electrolytes under anodic polarization.	6
2.2	Current density versus applied potential curve for the electrochemical etching of Si in an HF based solution, showing the regimes of pore formation and electro-polishing, the open-circuit potential (OCP) of the Si electrode is also shown.....	7
2.3	Schematic diagram of the standard anodization apparatus, the silicon wafer is mounted at the bottom of the cell	11
2.4	Cross sectional view of lateral and single cells	12
2.5	Cross sectional view of double tank anodization cell	13
2.6	Comparison of room-temperature photoluminescence spectra of (a) crystalline bulk silicon and (b) porous silicon, (logarithmic scale) [120,198].....	14
3.1	Experimental set-up of double tank cell.....	25
3.2	Schematic diagrams of new design Single tank cell	27
3.3	CAMAG UV-lamp (254-366) nm	32
3.4	Atomic Force Microscopy (AFM)	35
4.1	3-D AFM image of PS layer in designed single tank cell, with etching solvent HF: EtOH at ratio (1:1) in volume with different etching time used: (a) 10min , (b) 30min and (c) 60min	36
4.2	3-D AFM image of PS layer in double tank cell, with etching solvent HF: EtOH at the ratio (1:1) in volume with different etching time used: (a) 10min , b) 30min and (c) 60min	37
4.3	3-D AFM image of PS layer in designed single tank cell, at etching time 60 min. with different alcoholic etching solvents used : (a)HF: MeOH, (b) HF:EtOH, and (c) HF:PrOH , at ratio (1:1) in volume.....	39
4.4	3-D AFM image of PS two layers in designed single tank cell, etched with	

	HF: PrOH at ratio (1:1) in volume at etching time 60minute	40
4.5	3-D AFM image of PS layer in double tank cell, at etching time 60 min. with different alcoholic etching solvents used: (a)HF:MeOH, (b) HF:EtOH, and (c) HF:PrOH , at ratio (1:1) in volume.....	42
4.6	I-V measurement performed on prepared PS samples by using double tank cell (a)-(c), and designed single tank cell (d)-(f), with different etched time and constant current density $30\text{mA}/\text{cm}^2$	50
4.7	I-V measurement performed on prepared PS samples by using double tank cell (a)-(b), and designed single tank cell (c)-(d), with two different alcoholic solvents at current density $30\text{mA}/\text{cm}^2$ and etched time 60 min.....	51

LIST OF SYMBOLS AND ABBREVIATIONS

SYMBOL/ABBREVIATION

AFM	Atomic Force Microscopy
c-Si	Crystalline silicon
EELS	Electron Energy Loss Spectroscopy
EtOH	Absolute ethanol
HF	Hydrofluoric acid
IR	Infrared
IV	Current-Voltage measurement
MeOH	Methanol
NIR	Near Infrared
PL	Photoluminescence
PrOH	2-propanol
PS	Porous silicon
PSN	Porous silicon nanostructure
RT	Room Temperature
Si	Silicon
Si(OH) ₄	Orthosilicic acid
SiF ₆ ⁻²	Hexafluorosilicate ion
STM	Scanning Tunneling Microscopy
TEM	Transmission Electron Microscopy
UV	Ultraviolet
VIS	Visible

CHAPTER 1

INTRODUCTION AND OBJECTIVE

Silicon is the most important semiconductor for the electronic industry because of its availability in large area wafers with excellent quality and low cost, and the silicon based devices are so highly developed and constitute over 98% of all semiconductor devices sold worldwide [193,1]. But, its indirect band gap which lies in the near infrared (NIR), and low light emission quantum efficiency had limited its use in visible optoelectronics [2]. To date there is only one form of silicon that emits light efficiently which is called Porous silicon [119]. Porous silicon (PS) is a nanostructured material, which provides plentiful advantages to ace the present nano sized material community, as the name suggests Porous silicon is like a quantum sponge, containing a web like structure consisting of nanocrystallites and pores [7,3].

Since the remarkable discovery of visible photoluminescence (PL) at room temperature (RT) [194, 4], the observations of the blue shift of the absorption edge [2,5] and electroluminescence [6]. Porous Silicon has given considerable attention for a unique combination of properties, which are noticeable when its structure reduces to nanodimensions, these changes in properties are the outcomes of Quantum Confinement Effect [7], as could be seen in Figure 1.1.

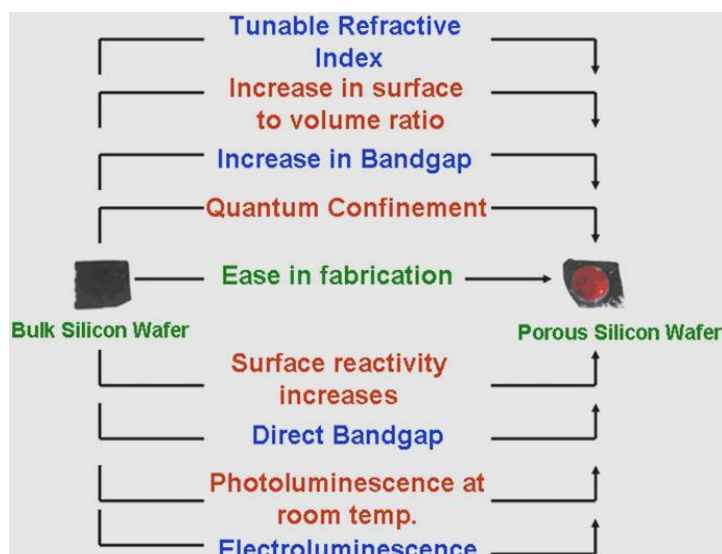


Figure1.1 Change of properties from bulk to Porous silicon [7].

Thus Porous silicon exhibits optical properties in emitting light efficiently (Light emitting diodes) and capability of guiding, modulating and detecting light [8]. Huge surface area up to $10^3 \text{m}^2 \text{cm}^{-3}$ and relatively high chemical activity makes it applicable for sensory technology [9, 10].

The design of *in vitro* and *in vivo* biomedical materials [11], properties for self reporting drug delivery (e.g., eye implants) [12]. Biocompatibility and most importantly the ability to degrade completely in physiological fluids into non-toxic orthosilicic acid ($\text{Si}(\text{OH})_4$), the natural form of Silicon found in the body known to be efficiently excreted from the body through the urine [11],[13-15].

The huge hydrogenated surface of Porous silicon allows applications of the material as a hydrogen reservoir, a component of fuel cells and H_2 gas sensors [16-18].

Porous silicon is formed by electrochemical etching (anodisation) where pore formation processes are assisted by an electrical current [9,10,19]. There are some variations of this process, such as the approach of current focusing [20], technique of internal current generation [21], patterning method [22], and light-assisted method [3].

Alternative Porous silicon preparation technologies are stain etching, based on the chemical reaction of crystalline silicon (c-Si) in a solution of hydrogen fluoride and nitric acid, or alkali [19],[23-25], Chemical vapor etching [26], plasma etching [27], photochemical (laser-induced) etching [28], Metal-assisted etching [29,30], spark processing [31], Micro and Nano-electrical discharge [32], combinational etching technique [33,34]. The material can be prepared in the form of a heterostructure [20-22], free-standing film [35], macro-or nanopowder [36-41], and nanowires [30, 42]. The morphology and porosity of the resulting Porous Silicon layers depend on [195]; the doping level, conductivity type, crystal orientation of the c-Si wafer [43], composition of the etching electrolyte, current density, anodization cells [10, 43].

In this study, a single tank electrochemical cell design has been successfully fabricated and compared with the standard cell (double tank cell). The systematic comparison include two main parameter ; the influence of anodization time with the electrochemical cell design, the influence of variable anodization electrolytes with the electrochemical cell design on the fabrication process of porous silicon nanostructures in p-type silicon. Morphology and pore formation of porous silicon layers were characterized by Atomic Force Microscopy (AFM) and current-voltage (I-V) measurement, photoluminescence emission by ultraviolet-lamp (254-366) nm. Three types of pores; mesopores, mesopores fill of mesopores, and macropore fill of mesopores have been obtained from designed single tank cell with (10,30 and 60) min. of anodization time ; whilst for double tank cell has been obtained with 60 min. of anodization time. Single tank cell has also been differentiated from double tank cell in showing stable red-orange ultraviolet photoluminescence emission with an improvement in current–voltage measurement.

A brief overview of the thesis is as follows:

In chapter 2 a detailed description of porous silicon formation process through; electrochemical etching of porous silicon, pore morphology, anodization parameters, photoluminescence of porous silicon, and historical overview through literature review of cells design and fabrication of porous silicon nanostructures.

Chapter 3 the main part of this thesis which concentrates on highlighting the structural differences between two types of electrochemical etching cells(double tank

and designed single tank cell) ; the effect of anodization parameters(cell design, electrolyte composition, anodization time) and characterization of the Porous silicon Nanostructures by Atomic force Microscopy (AFM);which has been employed mainly for the first time to study (the pore morphology of porous silicon in matter of its diameter, pore depth, kind of pores), current-voltage (I-V) measurement and CAMAG UV LAMP (254-366) nm.

Chapter 4 Discussion of the characterization results that have been obtained by Atomic force Microscopy, current-voltage (I-V) measurement and Ultraviolet photoluminescence emission of Porous silicon layers.

In the conclusion chapter, the summary of the results of the dissertation is presented and a future work for a potential research is foresighted briefly.

CHAPTER 2

FUNDAMENTALS OF POROUS SILICON FORMATION PROCESS

In this chapter, porous silicon formation process through electrochemical etching, pore morphology of the resulting porous layers, the main parameters which affect this process and the photoluminescence of the porous silicon have been described.

2.1 ELECTROCHEMICAL ETCHING OF POROUS SILICON

One of the intriguing reasons of the world-wide interest in Porous Silicon, It's easy, simple and low cost preparation technique [7, 44], which was first realized by Ulirs [45] and Turner [46]. Porous Si is a product of an electrochemical anodization of single Crystalline Si wafers in a hydrofluoric acid electrolyte solution [196]. The most appropriate technique to produce homogeneous porous layers and stable H-passivated surfaces is the electrochemical approach [6,47-52], which could be implemented potentiostatically or galvanostatically, functioning at a constant current is the most desirable by researchers which can guarantee a highly degree of controlling over porosity and thickness for the fabricated layers [53-58]. An anodization cell, silicon wafer (anode), a constant current source, platinum wire (cathode) and an electrolyte is the main constituents of an electrochemical anodization to produce porous silicon nanostructures. The electrolyte consists of hydrofluoric acid (HF, 48%) and ethanol [7,59,60]. The electrochemical cell should be made of HF-resistant material, like Teflon, the anodic current density can vary from 1 to 100 m A/cm² for a wide

anodization period, at higher anodic over potentials, electropolishing occurs and the surface becomes smooth and planar in morphology [53].

Figure 2.1 shows a cell which is known as the o-ring cell and could provide a reasonably homogeneous current density distribution on the silicon working electrode, copper or Aluminum plate is usually placed at the back side of silicon acting as a current collector and providing the electrical contact [53, 61, 62].

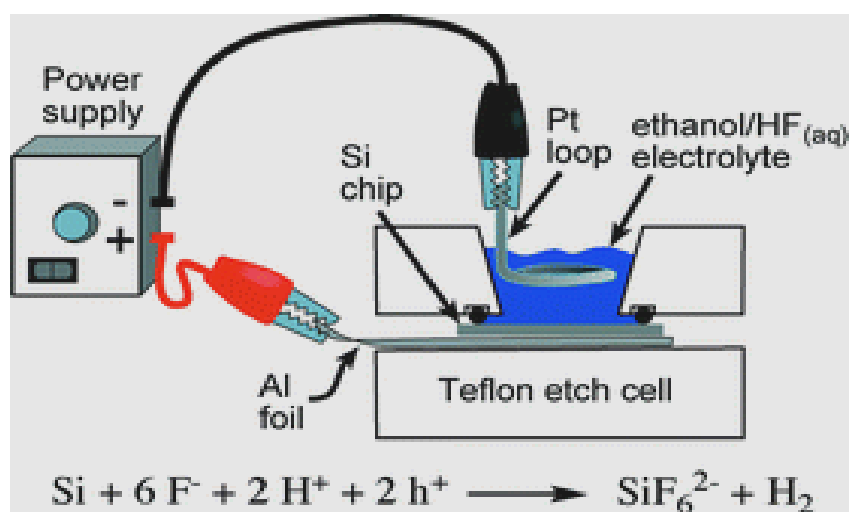
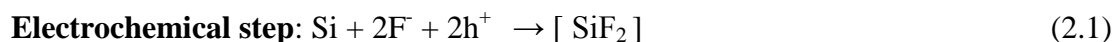


Figure 2.1 Schematic diagram showing Electrochemical cell used for the preparation of porous silicon in HF-based electrolytes under anodic polarization [53, 61, 62].

Before the electrochemical etching, it is essentially important to determine the most appropriate current density at which the pores are safely formed [53]. Figure 2.2 shows a typical current density-potential variation of the Si substrate while it was submerged in the anodizing solution, the curve displays a characteristic behavior of the Si/HF system using a moderately doped p-type Si in 1% HF solution, an initial exponential rise in current with applied potential that reaches a maximum value could be detected; three regions can be noticed from this curve; region (I) Pore formation which occurs at suitable current where porous layer is formed, region (III) Electropolishing which occurs at high potential values and formation of pores is not expected region (II) Transition region where pore formation and electropolishing process compete, the electrochemical etching of Si in an HF electrolyte in the regime of

pore formation, Figure 2.2 (region I), proceeds via a two- electron oxidation reaction according to the following equations[53]:



The net reaction of the two-electron process of Equation (2.3) predominates at lower potential and is the principal electrochemical reaction leading to the pore formation in Si, at high positive potential (electropolishing regime), the electrochemical etching of Si is running ideally involving a four-electron oxidation reaction with no pore formation, according to the following equation: [9 ,43, 53, 56, 59, 63].

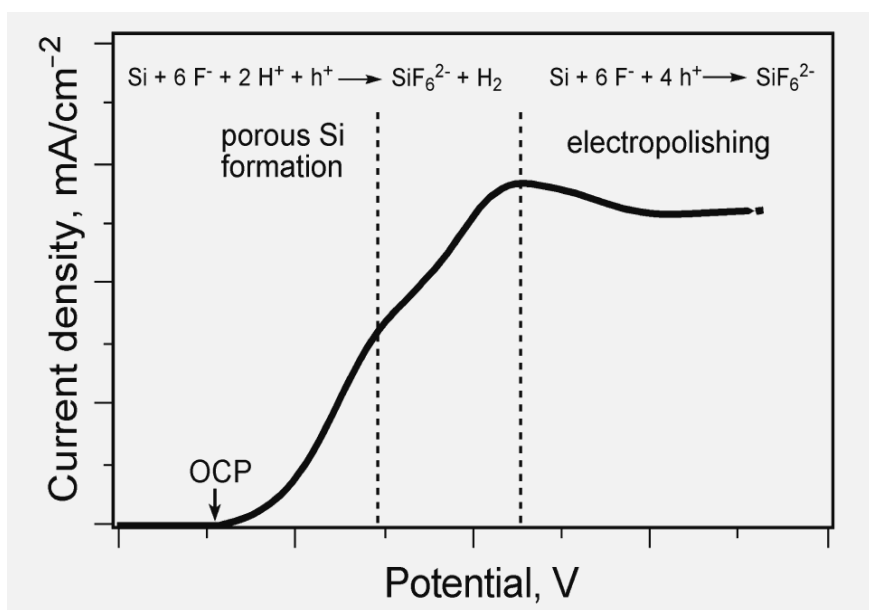


Figure 2.2 Current density versus applied potential curve for the electrochemical etching of Si in an HF based solution, showing the regimes of pore formation and electro-polishing, the open-circuit potential (OCP) of the Si electrode is also shown [53,63].

2.1.1 Pore Morphology

The morphology of PS has extremely rich details determined by the numerous factors involved in the electrochemical etching (anodization), p-Si and n-Si have distinct differences in the correlation between PS morphology and formation conditions [80]. Pore diameter is one of the morphological features of PS and can be defined depending on properties related to their shapes, size, branching (with no branches, with short branches, or with dendritic branches, or have no primary but densely and randomly branched pores [80]) and orientation [64, 65].

Different pore size regimes “according to the International Union of Pure and Applied Chemistry (IUPAC) Recommendations for the characterizations of porous solids” can be defined, Micropores have diameters smaller than 2 nm, Mesopores have diameters between 2 and 50 nm, Macropores have diameters larger than 50 nm [59, 66].

The diameter of pores and interpore spacing may vary with doping type and concentration, for heavily doped p and n types, ($> 10^{19}$); the pores have diameters typically ranging from 10 to 100 nm [197], for lowly doped p-Si ($<10^{15}$) the PS can have two distinct distributions of pore diameters: large pores with a distribution of diameters in the order of μm and small pores on the order of nm [80]. The pore diameter of p-Si of moderate or high doping concentrations decreases with increasing doping concentration [19], the effect of doping on pore diameter strongly depends on solution composition, potential and illumination conditions [80,67-70].

Pore diameter generally increases with increasing current density or potential and decreasing HF concentration [71]. The sensitivity of pore diameter to HF concentration strongly depends on solvent, a wider range of pore diameters can be obtained in organic solvents than in aqueous solutions [72-76].

The orientation of primary pores is in general in the $\langle 100 \rangle$ direction for all the PS formed on all types of (100) substrates [80] but very small pores < 10 nm do not show clear orientations [67, 77]. The macro pores formed on p-Si generally have smooth walls and an orientation toward the source of holes that is perpendicular to the surface, even on (110) and (111) samples [75, 78].

Depending on substrate orientation and formation condition [80], the shape of individual pores formed can be square, dendritic, circular, and star-like [67,79]. Individual pores depending on formation conditions, may propagate straight in the

preferred direction with very little branching or with formation of numerous side or branched pores [80]. The degree of branching and inter pore connection depends strongly on doping concentration, the most highly connected PS is found in the PS of lowly doped p-Si and the micro PS on illuminated n-Si [185,67].

The morphology of PS generally varies in the depth direction from the surface to the bulk [80]; there are two types of depth variations: 1) the change of pore diameter is gradual from the surface to the bulk where pore diameter is constant and 2) the change of pore diameter is abrupt from a surface layer to the bulk layer with a difference in diameter as large as three orders of magnitude [80].

The surface layer for the first type is a transition layer formed due to the transition from initiation of pores to the steady state growth [80], the thickness of the transition layer is related to the size of pores [69, 71, 80-84].

The second type is two-layer PS with a micro PS on top of a macro PS, two-layer PS forms only under certain conditions, for p-Si, two-layer PS are found to form on lowly doped substrates, for n-Si, formation of two-layer PS is associated with front illumination[80,73,74,78,85].

The PS formed on p-Si generally consists of micro pores, but when the resistivity is above a certain value macro pores can form underneath a layer of micro pores [80,68, 75,78] the resistivity at which this occurs, depends on type of solvent, HF concentration and current density, in aqueous HF solutions macro pores are found to form on substrates of resistivity higher than 5 Ωcm , on the other hand, macro pores has been found to form on substrate with a resistivity of 1 Ωcm in 2M HF + dimethylformamide electrolyte, presence of water in organic solvents tends to reduce the thickness of the micro PS layer [80], among all formation conditions doping concentration and solution composition appears to show the most clear functional effect on morphology [80,68, 73, 86-89].

2.1.2 Anodization Parameters

Silicon displays a peculiar electrochemical behavior in electrolytes containing hydrofluoric acid (HF) [90], when an anodic current is imposed, Nanometer-scale pores drill into the wafer, removing silicon in the form of the hexafluorosilicate ion (SiF_6^{-2}), the nanostructure that remains is a high surface area form of silicon which retains the crystallinity of the silicon wafer from which it was produced [90], probably the most

amazing aspect of this electrochemical system is that the porosity of a growing layer tracks the electrochemical current applied during the etch [90]. In here we are going to concentrate on the most important factors that rule this method.

2.1.2.1 Electrolyte

For the formation of the well-defined PS nanostructures with high aspect ratio, the major parameter for achieving this goal is the proper choice of the electrolyte [118] which include the HF-concentration, the supply of oxygen to the interface (which should be rather restricted) and the supply of reactive H (which should be large)[118]. Furthermore, the conductivity of the electrolyte, the viscosity and the stability of its components [118]. Due to the hydrophobic character of the clean Si surface, absolute ethanol is usually added to the hydrofluoric acid to minimize hydrogen bubble formation during anodization [91] and thereby improve layer uniformity. The ethanol is there primarily to reduce the surface tension of the electrolyte [59], allowing it to enter the very small pores as they are formed [59], other alcohols or water-miscible organic solvents can be used, though they can exert a profound influence on the pore morphology [59, 92, 93].

2.1.2.2 Potential

The anodization can be conducted either under galvanostatic or potentiostatic mode, however operation at a constant current is preferable as it gives a better control of the porosity for the fabricated layers [53]. It has been determined that the porosity of PS increases with increasing current density [99, 94, 95].

As porosity increases, the average pore size generally increases [99]. Increasing current density tends to increase the PS surface area, porosity, average pore size and pore size distribution [96-99].

2.1.2.3 Electrochemical cells

Anodization is performed in an electrolytic cell as shown in Figure 2.3, electrolysis is performed on a silicon wafer in a solution of hydrofluoric acid (HF) and ethanol with the silicon wafer acting as the anode. The cathode is a platinum electrode immersed in the electrolyte. When a current is induced through the solution and the

silicon wafer, the electrochemical reaction removes pores of silicon from the wafer leaving behind what is known as porous silicon [100]. The main problem which occurs during the etching is how to protect the back contact from the hazardous electrolytic solution and to prevent the current flowing directly from electrolyte to this contact disturbing the etching uniformity and hindering correct evaluation of current density [62,101]. Though careful design of the electrochemical cell is required to achieve good lateral PS film uniformity [44,102]. The electrochemical cell has been designed and made in various ways in the past.

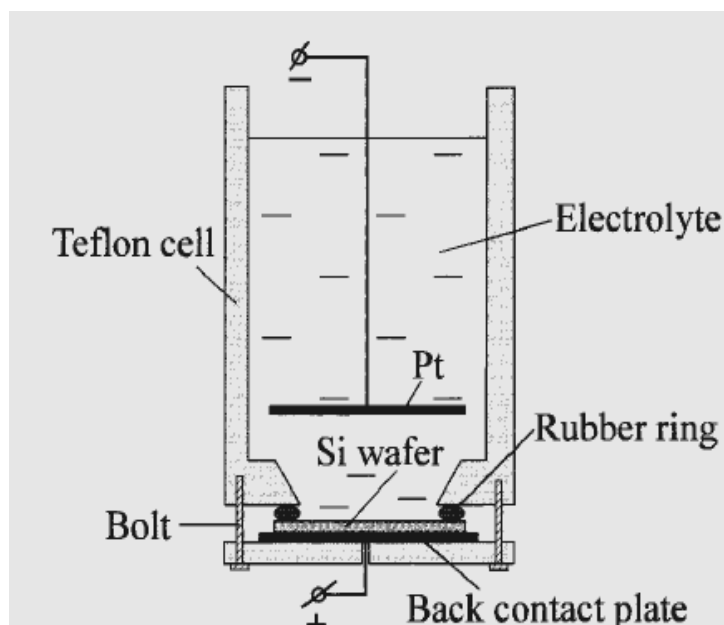


Figure 2.3 Schematic diagram of the standard anodization apparatus, the silicon wafer is mounted at the bottom of the cell [100].

The simplest electrochemical cell is a *lateral anodization cell* Figure 2.4 both the anode and cathode are placed vertically in the electrolyte and the current applied [99]; the Si wafer acts as the anode and the cathode is generally made of platinum or other HF-resistant and conductive material, The cell body is usually made of a highly acid resistant polymer such as Teflon, using this cell PS is formed all over the wafer surface exposed to HF [3], lateral anodization cell produces non uniform

porosity and thickness, due to a lateral potential drop which varies the local current density, therefore producing porosity and thickness gradients [3,45,46, 99,104].

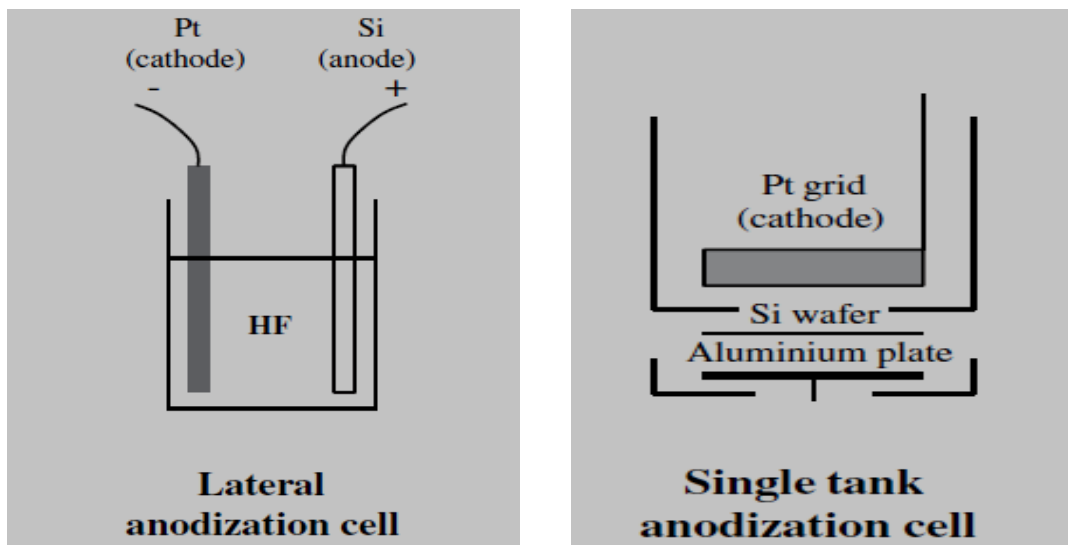


Figure 2.4 Cross sectional view of lateral and single cells.

The second type of anodization cell is *Single tank cell* Figure 2.4 in this cell, the Si wafer is placed on a metal disk and sealed through an O-ring, so that only the front side of the sample is exposed to the electrolyte. When a Si wafer with high resistivity (i.e. more than a few $m\Omega$ cm) is used, a high dose implantation on the back surface of the wafer is required to improve the electrical contact between the wafer and the metal disk. This cell is the most widely used because it leads to uniform PS layers, allows an easy control of both porosity and thickness, and it is suitable for front side illumination of the sample during the attach [53] [99, 101][105-108].

The third type of anodization cell is *the double tank cell* Figure 2.5 which uses electrolytic back side contact[99], two half cells are fitted with platinum electrodes with silicon wafer separating the half cells [99], the electrolyte is re-circulated using a pump which removes gas bubbles generated during etching and prevents any decreases in local HF concentration [99], the platinum electrodes are connected to a power supply and the current flows from one side to the other via the silicon wafer [99], [6,104,109-113].

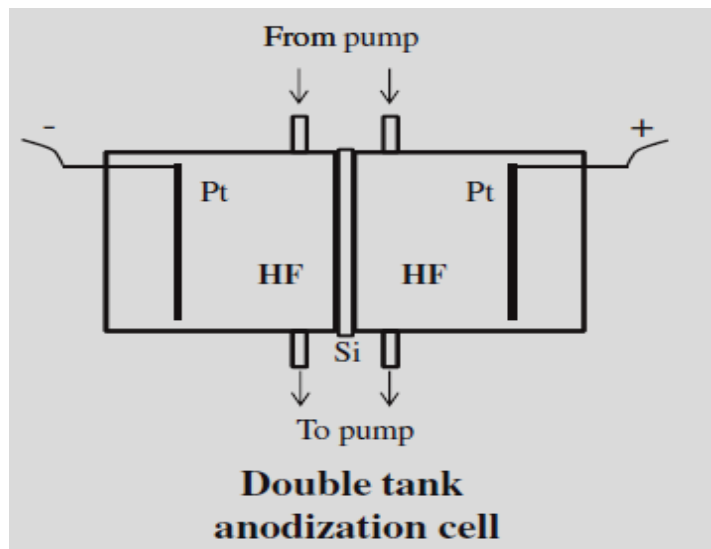


Figure 2.5 Cross sectional view of double tank anodization cell.

2.1.2.4 Anodization time

The period of time required to perform an anodization process, when a current is applied between a silicon wafer as an anode and a platinum electrode as a cathode, both the film thickness and porosity are directly proportional to the current density applied and they increase with increasing anodization time [114]. When the anodization time increases, both the thickness of porous layer and pore diameter increases [19],[115-117].

2.2 PHOTOLUMINESCENCE OF POROUS SILICON

Crystalline silicon is an indirect bandgap semiconductor with an energy gap of 1.12eV at room temperature, which is below the visible part of the electromagnetic spectrum[119], radiative recombination is only possible via absorption or emission of a phonon to maintain conservation of momentum[119], crystalline silicon structures in the nanometer size regime that are well passivated (either by hydrogen or oxygen) have shown an advantage over bulk crystalline silicon in suppressing non-radiative recombination events[119]. When the size of the silicon structures becomes small

enough ($\sim 3\text{nm}$) the band gap widens due to quantum confinement, pushing emission into the visible region [119].

Lehmann and Goesele [5,59] reported that electrochemical formation of porous silicon was intimately tied to the generation of nanometer-scale quantum wires and they showed that the optical absorption spectrum was consistent with a quantum confinement model. Canham [4,59] then showed that the material emits a bright red–orange photoluminescence, a clear indication that the optical physics of the porous silicon differs from bulk crystalline silicon, as shown in Figure 2.6

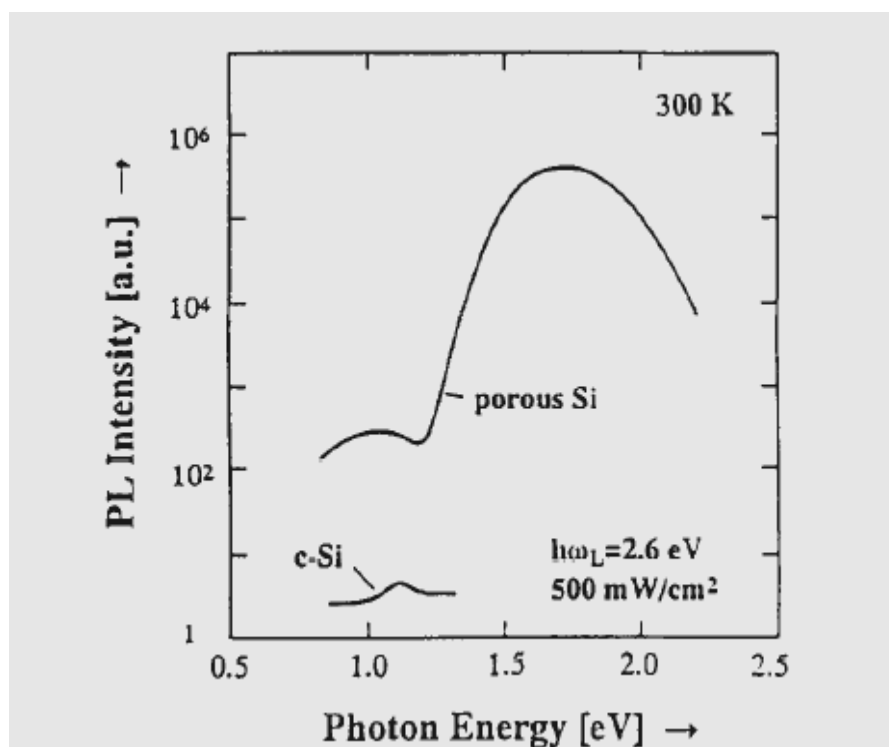


Figure 2.6 Comparison of room-temperature photoluminescence spectra of (a) crystalline bulk silicon and (b) porous silicon, (logarithmic scale) [120,198].

The origin of visible luminescence mechanism in nanoscale silicon is not as straightforward [119]; suggested mechanisms include carrier generation (or injection) and recombination in quantum confined silicon nanocrystals, interaction with surface states, the involvement of defect impurity luminescence centers, or combinations thereof [119]; two main mechanisms have been agreed on [119].

2.2.1 Pure Quantum Confinement

As silicon structure becomes confined by reducing the thickness in certain directions, the effective band gap increases [119]. The effective band gap of the material depends upon the confinement distance, dimensions that are confined, and the shape of the structures[119], according to the effective mass approximation the band gap of a material widens as $(1/d^2)$, where d is the confinement distance, the pure quantum confinement model was initially proposed by Canham [4,119].

In order to explain luminescence in porous silicon [119], and involves only carrier recombination within silicon nanocrystals; in this model, radiative recombination in a confined nanoscale silicon crystallite is more efficient than in crystalline silicon, the size of the silicon structures in visible light-emitting porous silicon is typically (20-30Å) where quantum confinement increases the energy band gap to $\sim 1.8\text{eV}$ [119,121,122].

2.2.2 Involvement of Surface States and Defect Centers

A model for luminescence which combines quantum confined nanocrystalline silicon with a surface state recombination emission process was proposed by Koch et al. [119,123]. This model differentiates between the crystallite core, which has an effective energy gap that considerably exceeds that of bulk Si due to quantum confinement, and surface states, which are electronic states in the disordered Si of the surface region[119]. The states are taken to be $\sim 0.3\text{eV}$ below the core states and are localized on a scale of 5-10Å [119]. Recombination can occur following trapping of one or both of the localized carriers in surface states within the energy gap [119].

Prokes et al. [119,124] have proposed a defect-based model for the visible light emission; their results indicate that red luminescence is directly correlated to the presence of oxygen-related centers (non bridging oxygen-hole center clusters), and that the emission process is due to energy transitions involving these defect centers. Because of strong supporting evidence for the different models, it is reasonable to assume that there may not be a unique origin of light emission [119]. Depending upon the materials processing, more than one light-emitting mechanism may be featured in luminescence spectra [119].

The photoluminescence spectrum of the porous layer and the luminescence color (which consider one of the intriguing properties of porous silicon) depend strongly on fabrication conditions, such as doping level and type (In higher resistivity (roughly 1 Ωcm) p-type material, the luminescence energy increases with increasing porosity), current density, solution concentration (the luminescence peak can be significantly altered by changing the composition of the electrolyte in which the samples are immersed. Using this approach the emission has been repeatedly cycled (> 100times) between green and red [199]).

Porous Si based structures have been reported to luminescence efficiently across the whole range from the near infrared ($\sim 1.5 \mu\text{m}$), through the visible region, and into the near UV [44]. Emission over such a broad spectral range arises from a small number of clearly distinct luminescence bands of different origin [44]. The four main types of photoluminescence phenomena observed from porous silicon samples are summarized in Table 2.1[59].

TABLE 2.1. Porous Si luminescence bands.

Spectral range	Peak wavelength (nm)	Luminescence band label
Ultraviolet	~ 350	UV band
Blue-green	~ 470	F band
Green-red	500-800	S band
Near infrared	1100-1500	IR band

The so-called ‘‘S-band’’ This band has been tuned across the entire visible range from deep red to blue [44,127]. The blue- green photoluminescence (PL) emission (the so-called ‘‘F band’’ due to its fast nanosecond decay time) was first reported by Harvey et al. [128]. Following the demonstration by Kovalev et al. [129] of quite strong PL output of this type from oxidized porous silicon produced by RTO treatment, the F-band has been the subject of several studies [44,130-134].

Infrared emission at room temperature was first achieved by Fauchet et al. for material annealed under ultrahigh vacuum (UHV) [135]. Ultraviolet emission was first reported by Jiang et al. [136] in 1993 from oxidized material under soft x-ray excitation [44, 137-141].

2.3 LITERATURE REVIEW

2.3.1 Cell design

Porous silicon is formed by electrochemical etching (Anodisation) Ulirs [45] in which he inadvertently noticed that electrolytic shaping is particularly well suited to making devices with small dimensions and discussed electrolytic etching can be conveniently divided into two topics-the choice of electrolyte and the method of localizing the etching action to produce a desired shape. He also explained the effect of cell designs and the effect of electrolyte during the etching process.

The simplest anodization cell, lateral anodization cell. Both the anode and cathode placed vertically in the electrolyte and the current applied [99]. The Si wafer act as the anode and the cathode generally made of platinum or other HF-resistant and conductive material [3,45, 99,102].

The second type of anodization cell was first realized by Turner [46] Single tank cell in this cell, the Si wafer placed on a metal disk and sealed through an O-ring, so that only the front side of the sample exposed to the electrolyte [3,46]. Grigoras and Pacebutas [101] which they had also developed a Single tank cell but the difference from the main design is the rubber ring that is placed over the silicon wafer and used to prevent the leakage of the HF solution.

The third type of anodization cell double tank cell which used electrolytic back side contact [99], two half cells fitted with platinum electrodes with silicon wafer separating the half cells [3, 6, 99,104, 105,111].

An interesting fabrication technique for porous silicon was proposed by Diaz et al. [100]. The main idea was not to immerse the sample into electrolyte, but only to

lower the holder into the Teflon container with HF solution until the silicon wafer made contact with the electrolyte surface. The contact was achieved by surface tension. They had used a metallic vacuum chuck connected to the vacuum line, and the silicon wafer with a metalized back was held by the vacuum suction [100,101].

Porous silicon fabrication technique for large area devices was proposed by Grigoras and Pacebutas [101]. Their set up was suitable for big wafers, using high anodization currents. The main part of their proposed electrochemical etching cell is a Teflon plate with drilled hole inside. This hole was used for air depumping from the cell and for pushing through a wire which connects the silicon sample to the current supply. Polyethylene pipe was fastened to the plate on the other side of the hole and connected to the vacuum pump. A small rotation for vacuum pump was used. Through the pipe and the hole in a plate a wire was pushed, on the end of which a soft contact spring was soldered. On the top surface of a Teflon plate a frame from a soft rubber was glued. It held the silicon wafer and protected the wafer's back contact from electrolyte electrically and mechanically. This cell used for PS coating of multicrystalline silicon solar cells.

An Electrochemical cell for the preparation of porous silicon proposed by Guerrero-Lemus et al. [171]. The main idea by using a silicon electrode holder, in which the silicon wafer pressed by means of copper badge toward a Teflon plug with a window to where the solution arrived, the silicon wafer centered in the plug by a circular rail, an O-ring impeded the infiltration of the electrolyte inside the silicon holder, as well as the chemical attack of the back metallization. The copper badge guaranteed a homogeneous contact to the back metallization of the silicon electrode.

2.3.2 Fabrication of Porous silicon Nanostructures

Electrochemical etching (Anodization) of silicon is usually performed in a hydrofluoric acid (HF) solution, and was first described by Uhler [45] and Turner [46] in the 1950's [185]. The first studies of this technique aimed at electropolishing silicon for use in semiconductor processing. However for certain parameters, a black film were produced, which later was observed to be a silicon mesh with highly interconnected pores: Porous Silicon.

Theunissen [142] showed that the interference colors were due to the formation of a porous structure within the silicon substrate due to selective etching. Since that time there have been a number of studies characterizing the properties of PS layers as a function of dopant type and concentration, electrolyte, and etching voltage or current [143]. Bulk Si wafers could be rendered visibly luminescent through anodization in the dark, or more rapidly using photoassisted etching [4,44,73,144].

White light illumination generally employed, either during anodization or post-anodization[44]. Illumination during anodization essential to generate luminescent PS in lightly doped *n*-type substrates [44,145].

Levy-Clement et al. [44,146] had undertaken detailed structural studies of the widely varying PS morphologies that could result from photo electrochemical (PEC) etching of such substrates. Ethanol frequently added to the hydrofluoric acid to minimize hydrogen bubble formation during anodization and thereby improve layer uniformity [44,91].

Beale et al. [147-149] studied the formation properties of the PS and its applications had been focused on dielectric isolation for silicon-on-insulator structures in the 1980's. While PS layers fabricated in concentrated (40–50 wt %) aqueous HF could be wholly micro porous [44,150]. It was difficult to avoid the formation of macro pores under such conditions if relatively thick PS layers were fabricated and pronounced in homogeneity with depth (porosity gradients) can be a characteristic feature of such material [44,151]. The diameter of PS layer pores or channels was found to range from 1 up to 100 nm associated with porosities of 20-80%. The channels in non degenerated *p*-type silicon were found to be the smallest (typically around 2 nm) [5,148,152].

Canham [4] had suggested that the selective etching process could be used to fabricate Silicon quantum wire arrays. Porous silicon formation through a quantum wire effect was studied by Lehmann and Gosele [5], in which they showed that formation of PS layer on non degenerated *p*-type silicon self-adjusting process due to a geometrical quantum well or wire effect associated with the thin silicon walls remaining between the pores.

Porous silicon formation mechanisms review by Smith and Collins [67], in which they discussed thoroughly the surface dissolution chemistry, inter-facial potential distribution and pore formation conditions, pore morphologies and PS formation models:

- (A) The Beale model
- (B) The diffusion-limited model
- (C) The quantum model

Cullis and Canham [153] observed column like structures with cross-sectional diameters of less than 3 nm in light emitting porous Si by transmission electron microscopy (TEM). Cole et al. [154] studied Si microcrystals of few nanometers in diameter by high-resolution TEM. Nishida et al. [155] also observed a particle like Si structure of several nanometers to several tens of nanometers by high resolution scanning electron microscopy. Nakajima et al.[156]examined the microstructure of luminescent PS by cross-sectional high-resolution transmission electron microscopy and found a thread like-structure consisting of Si microcrystals, also found Si microcrystals with sizes ranging about 3-20 nm randomly distributed throughout the porous silicon.

Weng et al. [157] reported Luminescence studies on PS, in which they observed a red shift process of luminescence wavelength in an as-prepared PS layer, Si-H bonds of a significant concentration are gradually replaced by Si-O bonds when PS was exposed to air at room temperature, which coincides well with desorption of hydrogen from the silicon surface.

A microstructural study of porous silicon investigated by Berbezier and Halimaoui [158] in which they obtained (PS) films from lightly and heavily doped p-type silicon had been investigated by transmission electron microscopy. Silicon crystallites with nanometric dimensions had been evidenced in both types of PS layers. High resolution observations revealed lattice disorder even for low-porosity (65%) samples. Concerning PS layers obtained from lightly doped substrates, it was shown that increasing porosity leads to a crystallite size reduction and to the deterioration of the material crystalline. When the porosity was increased up to a value of about 85%, silicon crystallites with a mean diameter of less than 3 nm and an amorphous phase were clearly imaged.

Simple particle-in-a-box calculations showed that, for particle sizes of the order of nm, optical band-gap widening occurred for semiconductors such as silicon: the corresponding bulk mean free path for electrons in silicon is about 10 nm. Band-gap widening had been observed in several nanostructured systems. One such system is PS by Kalkhoran et al. [159].

Layer microstructure sensitive to many parameters which need to be controlled during etching[44]. These include not only electrolyte composition, current density and applied potential but also electrolyte temperature if excellent reproducibility from run to run had to be achieved [44,160].

Luminescent porous Si layers generated in either dilute aqueous HF or ethanoic HF were generally mesoporous [44,66].

Anodization under galvanostatic conditions generally the preferred approach for reproducibly attaining wide ranges of porosity and thickness [44]. Careful design of the electrochemical cell required to achieve good lateral film uniformity, as succinctly discussed by Halimaoui [44,102].

Porous silicon: a novel material for Microsystems by lang et al. [105] had shown PS had a number of interesting features which open the way to new processes and devices in silicon technology.

Micromaching applications in Porous silicon by lang et al. [161] in which they described the most common micromachining applications, free-standing membranes, cantilevers and bridges were needed[161]. In contrast to the surface micromachining method, where a thin film of silicon dioxide ($< 10 \mu\text{m}$) dissolved as a sacrificial layer, by means of PS technology, thick sacrificial layers can be produced (up to $100 \mu\text{m}$), these results - after their dissolution - in a high distance of membranes and bridges to the bulk silicon, an important aspect for the sensitivity of thermal transducers [161].

The relation between the visible and the infrared luminescence bands in porous silicon comparison with amorphous Si alloys by Petrova-Koch and Muschik [162], they summarized the results published in the literature, an empirical correlation between the energy position of the IR and the VIS PL bands in PS had been shown in their paper [162].

A review by Delerue et al. [163] which they discussed thoroughly the calculations of the energy gap vs. size predicted radiative recombination times and the importance of phonon-assisted transitions, followed by an analysis of the influence of defects surface dangling bonds and donor or acceptor impurities, the excitonic exchange splitting as a function of the shape of crystallites, through a theoretical description of porous silicon [163].

Characterization of porous silicon-on-insulator films prepared by anodic oxidation by Lee et al. [164], techniques for controlling the growth of the bottom oxide formed by simple electrochemical oxidation of PS films were explored and the resulting porous silicon-on-oxide structures were characterized [164]. The thickness, uniformity, and density of the bottom oxide layer can be adjusted by selecting the PS morphology and controlling the conditions of oxide formation [164].

EELS investigation of luminescent nanoporous p-type silicon by Berbezier et al. [165] sample of 80% porosity obtained by electrochemical dissolution in HF-based solutions by electron energy loss spectroscopy EELS inside a transmission electron microscope TEM [165].

The discovery of macropores in p-type Si [75, 78, 166] which according to the space charge region model, “should not occur”, made clear, however, that space charge region effects were not the only decisive factor for the formation of macropores [167]. In a more comprehensive view, pore formation could be seen as belonging to the class of ‘critical phenomena’, and space charge region effects were one of several mechanisms that tend to synchronize current flow in time and space and thus induce current oscillations and pore formation [167].

Christophersen et al. [118] studied macropore formation in moderately doped p-type Si in mostly galvanostatic experiments ($2\text{--}10\text{ mAcm}^{-2}$) with various fluoride containing electrolytes and substrate orientations [(100), (511), (5 5 12), (111)] from the nucleation phase to the phase of stable pore growth [118]. The most important parameter of the electrolyte was its ability to supply oxygen and hydrogen [118]. Whereas oxygen necessary for smoothing the pore tips, hydrogen is the decisive factor for the anisotropic growth and the passivation of macropore side walls [118]. Based on a better theoretical understanding of the electrode processes in general pore formation in

particular, etching conditions could be optimized for the generation of macropores in p-type Si with better aspect ratios, better stability, and smaller diameters than those in n-type Si in their titled paper [118] “Crystal orientation and electrolyte dependence for macropore nucleation and stable growth on p-type Si”.

A detailed review titled Formation and application of porous silicon by Föll et al. [10] explained all manifestations of pores in silicon with particular emphasis put on macropores with respect to possible applications.

Christophersen et al. [168] studied the influence of different organic electrolytes on the electrochemical reactions and the morphologies of macroporous silicon[168]. In their entitled paper Organic and aqueous electrolytes used for etching macro and mesoporous silicon.

A new type of HF solution [2]; HF-acetonitrile (MeCN) had been employed to produce 10–30 μm thick (PS) layers by photo electrochemical etching of different types of Si wafers, Si (100), Si (111) and polycrystalline Si, with different resistivities studied by Feng et al.[2] In their entitled paper “Combined optical, surface and nuclear microscopic assessment of poroussilicon formed in HF-acetonitrile.

A paper confirmed [169] the possibility of porous silicon formation in the dark and with backside illumination, these being Alternative methods for topside assisted illumination etching methods by Jakubowicz [169] in which the properties of porous silicon prepared at different illumination and electrochemical conditions were studied [169].

Fast speed nano-sized macropore formation on highly-doped n-type silicon via strong oxidizers by Ge et al. [170] the growth of nano-sized macropores at high speed is studied in their work The fabrication of porous silicon (PS) layers based on the crystalline silicon wafer n-type of (100) orientation using electrochemical etching process was conducted[170].

The effect of various etching times on the structural and optical properties of the PS layers was investigated by Salman et al. [117] in their paper Effect of Etching Time on Porous Silicon Processing.

Hydrogen-terminated porous Si wafers with (100) and (111) oriented crystal planes were fabricated through a photo-electrochemical etching [106]. It is found that the porosity of silicon wafers and their etch rates are determined as a function of crystal orientation [106]. Due to the anisotropic etching behavior of Single-crystal silicon, the hydrogen-terminated porous Si (100) wafers exhibited not only more excellent photo degradation activity but also stronger stability for methyl orange degradation than hydrogen terminated porous Si (111) wafers under visible light irradiation, an investigation performed by Xu et al. [106].

CHAPTER 3

DESIGN, FABRICATION AND CHARACTERIZATION OF POROUS SILICON NANOSTRUCTURES (PSN)

The electrochemical anodization of p-type silicon has been thoroughly investigated in this chapter ; this investigation include the influence of the main anodization parameters on the fabrication process of porous silicon nanostructures in p-type silicon, which include cell design, current density, electrolyte composition and anodization time. Our focus in this chapter will be through highlight the structural differences between two types of electrochemical etching cells and the effect of anodization parameters. A detailed description of the characterization techniques which have been used in this work which include; Atomic Force Microscopy (AFM) and current-voltage (I-V) measurement, photoluminescence emission by ultraviolet-lamp (254-366) nm.

3.1 THE CHEMICALS

The following chemicals have been used in the present work.

- i. Hydrofluoric Acid (Sigma Aldrich 48 wt. % in H₂O \geq 99.99%).
- ii. Ethanol (Sigma Aldrich, 99.9%).
- iii. Methanol (Sigma Aldrich, \geq 99.9%).
- iv. 2-Propanol (Sigma Aldrich, 99.9%).
- v. Pentane (Sigma Aldrich, \geq 99%).
- vi. Ultra pure water.

3.2 MATERIALS AND CONSTRUCTION

The electrochemical etching cell is the centre part for the fabrication of porous silicon nanostructures PSN, through the cell designs, different sizes and shapes of pores can be obtained. The material used to construct the etch cell is Teflon [59], which is resistant to HF and organic solvents [59]. In the present work we have used two electrochemical cells design.

3.2.1 Double Tank Cell

Which has been used as the standard etch cell for producing porous silicon nanostructures in the department of Electrical and Electronics Engineering Figure 3.1, this cell consists of a double tank in which the electrolyte of one of the tanks is used as a back side contact of the silicon wafer. The cell body is a square section Teflon recipient which is resistant for Hydrofluoric acid (HF). The double-tank cell consists of two half-cells in which the silicon wafer is used to separate the half-cells and isolate them from each other, the back side of the Si wafer acts as a Secondary cathode where the proton reduction takes place leading to hydrogen evolution, the front side of the wafer acts as a secondary anode on which the porous silicon is formed[102].



Figure 3.1 Experimental set-up of double tank cell.

The electrolytic contact avoids the usual back-metallization of the silicon wafers before etching, and reduces the non uniformities commonly observed because of this back side metal contact, and produces a more uniform porous silicon layer. This cell doesn't have a cover considered as an open cell, the result of that will be an evaporation and temperature changes of the electrolyte. The volume of this cell is 50ml of electrolyte.

3.2.2 Single Tank Cell

This cell has a lot of structural differences than the double tank cell. There are many successful single tank cell designs but we have designed a single tank cell that have some improvements to the cell designs in the literature and that best suits our project purposes, the designed single tank cell has the following adjustments:

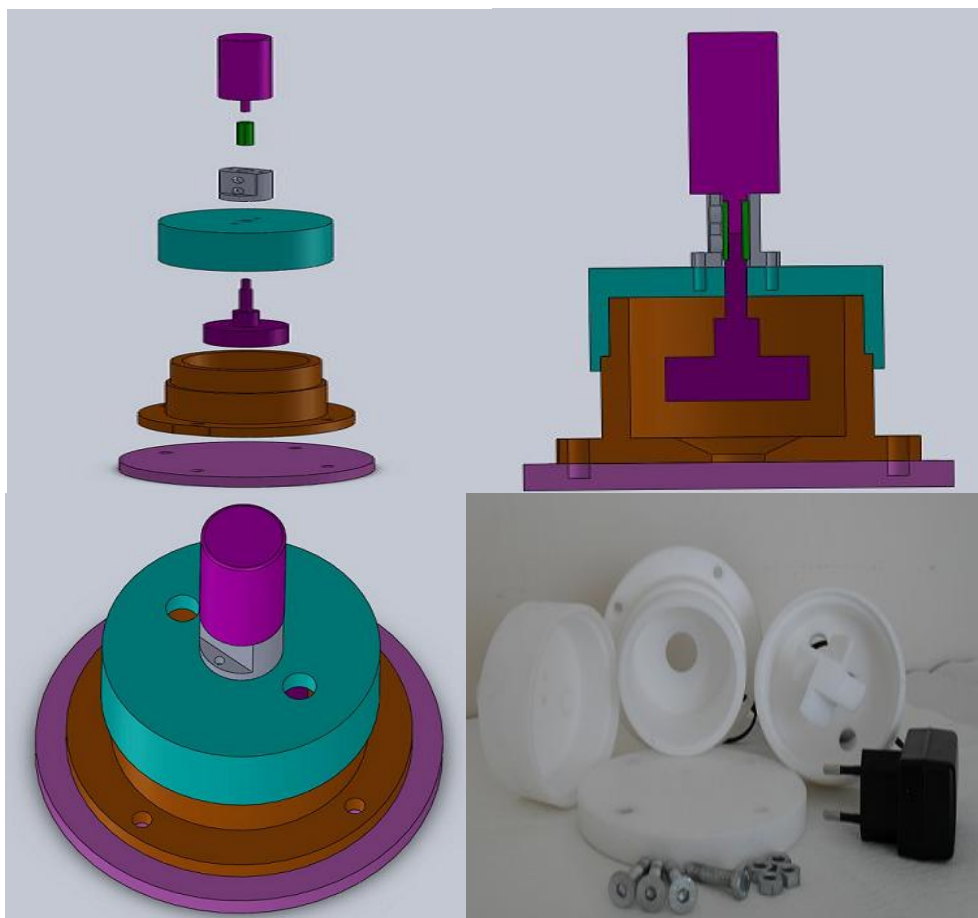


Figure 3.2 Schematic diagrams of new design Single tank cell.

1. This is a cylindrical section body cell type the Si wafer is placed on a metal disk at the bottom of the cell, sealed through an O-ring, so that only the front side of the sample is exposed to the electrolyte. The Si wafer connects through the metal sheet is acting as anode (working electrode) and the platinum electrode acts as a cathode (counter electrode). To obtain a uniform porous layer it's important for the counter electrode to be lying in a plane parallel to the silicon wafer and fully immersed in the HF electrolyte [59].
2. The nominal area of exposed silicon with this cell design is 6.15 cm^2 which is considered as large etch cell and the volume required for this cell is 60ml of electrolyte and very suitable for all research scale experiments.
3. This cell has two different movable covers, one with electrical stirrer and the other without stirrer with this covers come the benefits of:
4. Maintaining the temperature and quantity of the electrolyte during the electrochemical reactions.
5. The height of the covers could be changed in that way we can adjust the height of the electrode to the desired and suitable height. We have adjusted it for 3 cm distance from the etching area for our experiments. Also the ability to change the location of the electrodes as the cover has provided with two openings for this purposes.
6. The function of the electrical stirrer is to stir the electrolyte and remove hydrogen bubbles in case of the composition of the electrolyte has de ionized water.
7. These covers have two apertures for illumination in case of n-type silicon wafer.
8. The health effects due to HF gas evaporation will be reduced.

3.3 POWER SUPPLY

Electrochemically etched porous silicon samples are usually prepared under controlled current conditions meaning the feedback loop is rather set to hold up the current rather than the voltage constant [59]. The current source we have been used in our experiments is Keithley2200-60-2 (Programmable DC power supply. 60 V, 2.5 A, 1 channel, USB, GPIB).

3.4 PREPARING A SILICON WAFER

There are three properties defining crystalline silicon wafers: The cut (crystal orientation) of the wafer, dopant type, and resistivity, all three parameters are crucial in determining the type of Silicon Nanostructures [59], we are going to be obtained. The properties of Silicon wafers we have used in present work as following:

- i. Orientation: $\langle 100 \rangle$, polished on (100) face.
- ii. Type/dopant: P-Boron, Boron is the dopant.
- iii. Resistivity: The electrical resistivity of the wafer, (1-10) Ωcm .
- iv. Cleaving the silicon wafers: When cleaving the silicon wafers the orientation of the wafers should be put in consideration for p-type (100), there are 2 flats, the major flat is parallel to the (110) cleavage plane, the second flat is 90° from the major flat.
- v. Cleaning process of silicon wafers: A quick dip 15 s in low concentration (5%HF) solution to remove the native surface oxide and some organic residues.

3.5 ELECTROLYTE

The electrolyte used for the fabrication process of porous silicon nanostructures is an aqueous dilution of Hydrofluoric acid (HF) 48%. The dilution is necessary due to the hydrophobic character of the clean silicon surface. In fact ethanoic solutions infiltrate the pores; on the contrary pure aqueous HF solutions do not. This is very important for the lateral homogeneity and the uniformity of the porous silicon layer in depth. Moreover, the lateral homogeneity and the surface roughness can be reduced by increasing the electrolyte viscosity. Hydrogen terminated porous silicon is fairly hydrophobic[59], water does not wet the pores very well, the ethanol is there primarily to reduce surface tension of the electrolyte allowing it to enter the very small pores as they formed (3, 172,173).

3.6 THE ELECTROCHEMICAL CELLS

Two types of electrochemical cells have been used in this investigation, these were termed Double and Single tank cells as will be described in the following sections (3.6.1, 3.6.2, 3.6.3, & 3.6.4) to fabricate porous silicon nanostructure (PSN).

3.6.1 Double Tank Electrochemical Cell

In this set up we have prepared porous silicon samples from p-type silicon.

The double tank cell has been used, with the nominal etching area is 0.785cm^2 , a boron doped, p-type, polished (100) silicon wafer with a high resistivity (1-10) $\Omega\text{ cm}$ cut to $2 \times 2\text{ cm}^2$. Prior to etching the wafer has been cleaning by removing the native oxide in a low concentration HF (5 wt. %) solutions for a few seconds. The etching solution consists of HF (48 wt. %) electrolyte and absolute ethanol (EtOH) at ratio (1:1). The electrode distance from the etching area is 4 cm. The power supply set in constant current mode (galvanostat) has delivered a constant current density of 30 mAcm^{-2} , for times (10, and 30) minutes.

3.6.2 Single Tank Electrochemical Cell

In this set up we have prepared porous silicon nanostructures samples from p-type silicon. The new designed Single tank cell has been used with the nominal etching area is 6.15cm^2 , a boron doped, p-type, polished (100) silicon wafer with a high resistivity (1-10) $\Omega\text{ cm}$ cut to $4 \times 4\text{cm}^2$. Prior to etching the wafer has been cleaning by removing the native oxide in a low concentration (5%) HF solutions for a few seconds. The etching solution consists of HF (48 wt. %) electrolyte and absolute ethanol (EtOH) at ratio (1:1). The electrode distance from the etching area is 3cm the location of the platinum electrode has a central location to the Si wafer. The power supply set in constant current mode (galvanostat) has delivered a constant current density of 30 mAcm^{-2} for time (10, and 30) minutes.

3.6.3 Double Tank Electrochemical Cell

In this set up we have prepared porous silicon samples from p-type silicon.

The double tank cell has been used, with the nominal etching area is 0.785cm^2 , a boron doped, p-type, polished (100) silicon wafer with a high resistivity (1-10) $\Omega\text{ cm}$ cut to $2\times 2\text{ cm}^2$. Prior to etching the wafer has been cleaning by removing the native oxide in a low concentration (5%) HF solutions for a few seconds. The etching solutions were a mixture of aqueous HF (48 wt.%), and the following alcohols at ratio (1:1) in volume: methanol (MeOH), ethanol (EtOH), and 2-propanol (PrOH). The electrode distance from the etching area is 4 cm. The power supply set in constant current mode (galvanostat) has delivered a constant current density of 30mAcm^{-2} , for 60 minutes.

3.6.4 Single Tank Electrochemical Cell

In this set up we have prepared porous silicon nanostructures samples from p-type silicon. The Single tank cell has been used with the nominal etching area is 6.15cm^2 , a boron doped, p-type, polished (100) silicon wafer with a high resistivity (1-10) $\Omega\text{ cm}$ cut to $4\times 4\text{cm}^2$. Prior to etching the wafer has been cleaning by removing the native oxide in a low concentration HF (5 wt.%) solutions for a few seconds. The etching solutions were a mixture of aqueous HF (48 wt.%), and the following alcohols at ratio (1:1) in volume: methanol (MeOH), ethanol (EtOH), and 2-propanol (PrOH). The electrode distance from the etching area is 3cm the location of the platinum electrode has a central location to the Si wafer. The power supply set in constant current mode (galvanostat) has delivered a constant current density of 30mAcm^{-2} for 60 minutes.

3.7 CHARACTERIZATION OF POROUS SILICON NANOSTRUCTURES

3.7.1 CAMAG Ultraviolet LAMP (254-366) nm

UV lamp for two wavelengths 254 and 366 nm, 2 light tubes 8 W each. This UV lamp can be lifted and directed to any object as shown in Figure 3.3. The two types of UV light are used:

- i. **Long-wave UV 366 nm** : Under long wave UV light fluorescent substances appear as bright, often differently colored zones on a dark background. This detection method is more sensitive, the higher the UV

luminance is, the more effective the visible light components are filtered out and the more effective external light is shielded.

- ii. **Short-wave UV 254 nm** : 254 nm appear under UV, absorb UV light of this wavelength substances as dark areas on a light background, as long as the layer contains a corresponding fluorescent indicator F254.



Figure 3.3 CAMAG UV-lamp (254-366) nm

3.7.2 Atomic Force Microscopy (AFM)

The atomic force microscope (AFM) was invented in 1986 by Binnig et al. [174], the same year in which Binnig and Rohrer won the Nobel Prize for Physics for developing the scanning tunneling microscope (STM). Binnig et al. essentially combined the principles of the STM and the stylus profilometer to create a characterization tool that incorporates a probe that does not damage the sample.

Atomic force microscopy (AFM) is an imaging technique used to determine topography and other properties of surfaces. It is an important tool for nano science. Capable of using and measuring van der Waals forces, AFM is a new super-resolution near-field probe microscopic technique that can be applied to both conductors and insulators[177].

AFM can provide *in situ*, real-time, real-space and high-resolution images of the sample surface[177]. AFM can also provide dynamic three dimensional images of the

sample surface and quantitative information and thus transcends the planar imaging of other instruments[177]. Compared with other current surface analysis techniques, AFM has the advantage of low requirements for sampling procedures and working environment. As a tool for measuring the surface physical properties of various samples [175-177].

AFM provides a 3D profile of the surface on a nanoscale, by measuring forces between a sharp probe (<10 nm) and surface at very short distance (0.2-10 nm probe-sample separation). The probe is supported on a flexible cantilever. The AFM tip “gently” touches the surface and records the small force between the probe and the surface. Probes are typically made from Si₃N₄ or Si. There are 3 primary imaging modes in AFM [178]: Contact AFM: < 0.5 nm probe-surface separation; intermittent contact (tapping mode AFM): 0.5-2 nm probe-surface separation

Non-contact AFM: 0.1-10 nm probe-surface separation.

Even though AFM is widely used in other fields, but it has been scarcely used to study the pore morphology of porous silicon in matter of its diameter, pore depth, kind of pores. It has been employed as a partial tool to study the surface roughness. Tsai et al. [179] observed that the decrease in lateral feature size coincides with an increase in porosity which would be consistent with a strong correlation between the AFM results and an average pore size.

Song et al. [180] studied the morphology of the porous layers by using AFM. They found that the surface was covered with a dense porous layer of hillocks and holes[180].

The AFM system consist of a mechanical and sound vibration isolated main probe station, power control and light bank units. It is operated by a data acquisition and the images are processed by graphics software. In the present work (Atomic Force Microscopy) is PARK SYSTEM THE XE -100 contact mode has been used , Figure 5 shows the device main components.

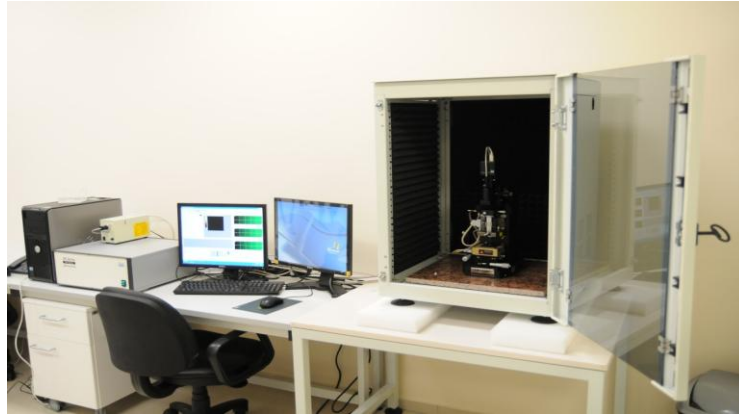


Figure 3.4 Atomic Force Microscopy (AFM).

3.7.3 Current-Voltage Characteristics

Keithley Semiconductor characterization system model 4200-scs was used to measure current-voltage characteristics.

CHAPTER 4

DISCUSSION OF THE CHARACTERIZATION RESULTS

4.1 ATOMIC FORCE MICROSCOPY

The morphology of PS samples (pore size and type) examined by Atomic force microscopy (AFM). Figure 4.1(a)-(c) and figure 4.2(a)-(c), show three dimensions AFM images (500 nm x 500 nm) of porous silicon layers with ethanolic anodization electrolytes at three anodization times, while figure 4.3(a)-(c), figure 4.4 (a)-(b) and figure 4.5(a)-(c) show three dimensions AFM images (500 nm x 500 nm) of porous silicon layers prepared with three alcoholic anodization electrolytes at constant anodization time of 60 min., and current density of $30\text{mA}/\text{cm}^2$ with two electrochemical cells design. AFM can determine the surface nature of samples under contact mode employing section analysis [177]. Section analysis analyzes a profile of the scanning area of the sample, revealing the undulating vertical distance and surface roughness along the section, and thus measures the diameter and depth of pores [115,175,177,180].

Figure 4.1(a)-(c): Shows the AFM images of PS samples fabricated by designed single tank cell with (10,30,60) min. as an anodization time ; which reflect a surface covered with a dense porous layer of hillocks and holes [48], with spongy morphology could be obtained with three etching times. By manually analyzing each image profile of the figure 4.1(a)-(c) we could have obtained different sizes of pores on PS layer. The diameters and depths of pores of sample etched at 10 min. were: *meso pores* between (6-40) nm, and (0.2- 0.54) nm, respectively and *meso pores fill of meso pores* (27-49)

nm, (0.53-1) nm, respectively. For 30 min. sample diameters and depths of pores were: *meso pores* between (6-20) nm, and (0.2-1.1) nm, respectively; *meso pore fill of meso pores* (25) nm, and (0.4)nm, respectively and *macro pore fill of meso pores* (61)nm, and (1.1)nm, respectively.

For 60 min.were: *meso pores* between (9-37)nm, and (0.3-1.25)nm, respectively; *meso pores fill of meso pores* between (24-45)nm , and (1.25-1.63)nm, respectively; and *macro pore fill of meso pores* (63)nm, and (0.9)nm, respectively

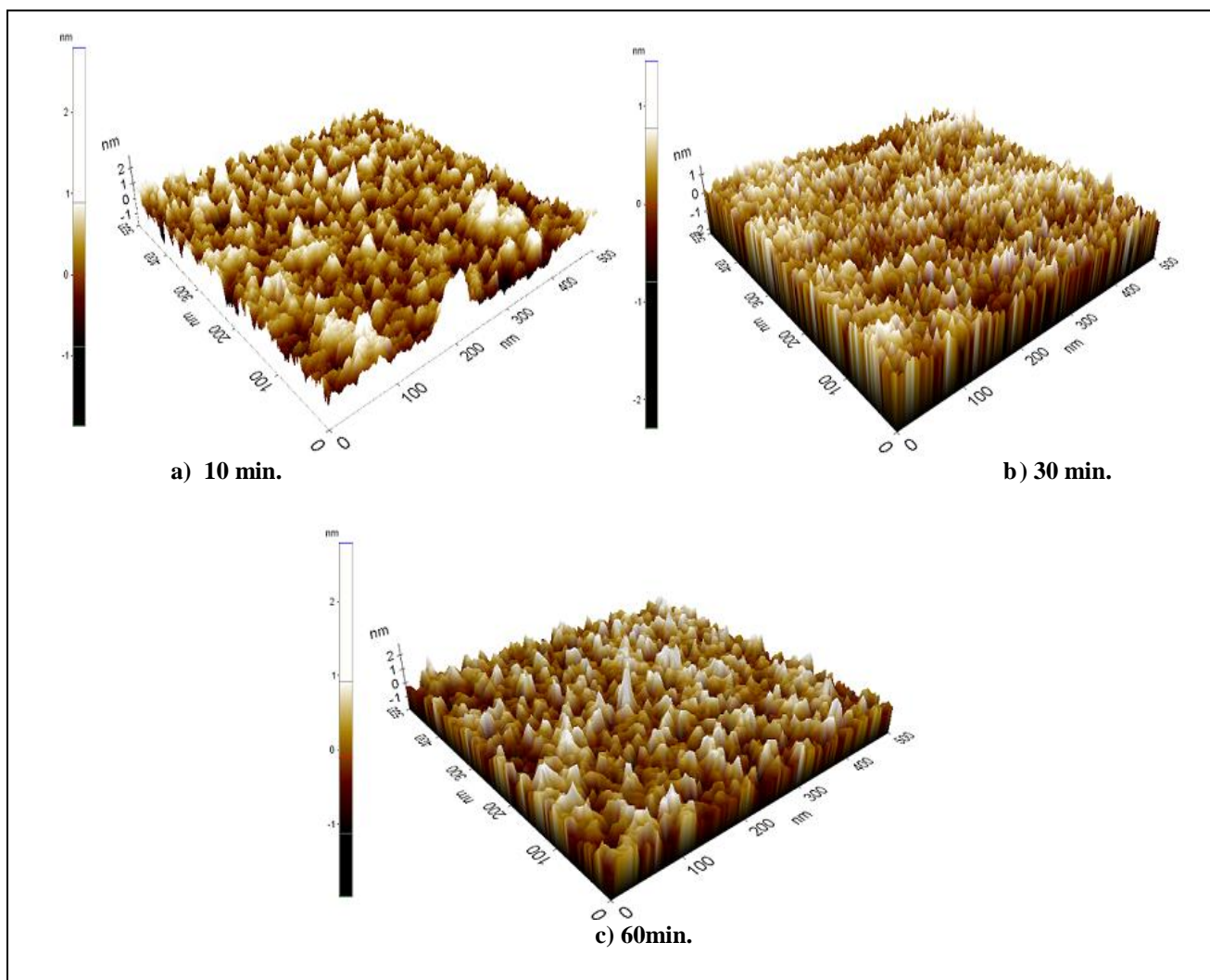


Figure 4.1 3-D AFM image of PS layer in designed single tank cell, with etching solvent HF: EtOH at ratio (1:1) in volume with different etching time used: (a) 10min , (b) 30min and (c) 60min.

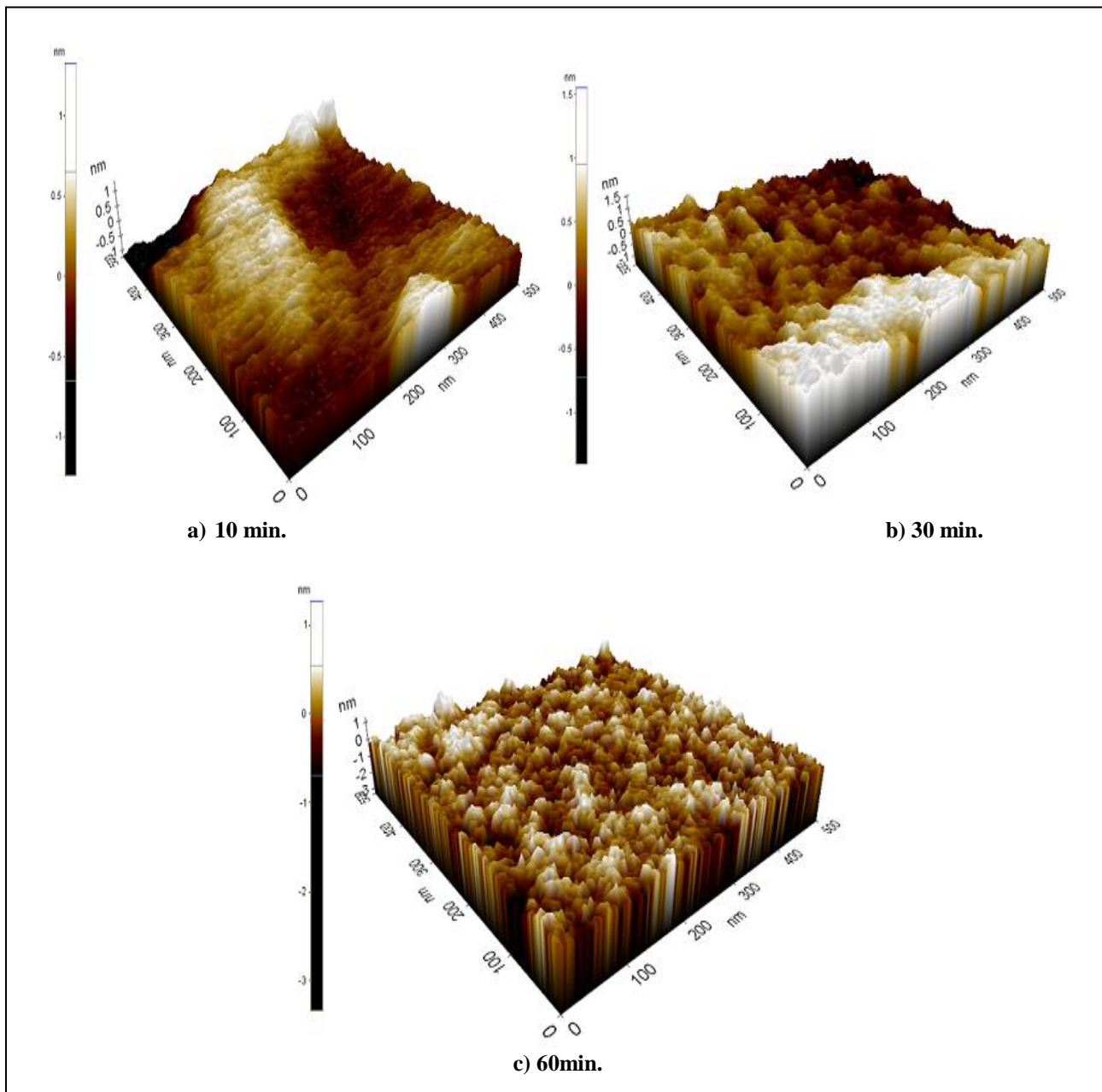


Figure 4.2 3-D AFM image of PS layer in double tank cell, with etching solvent HF: EtOH at the ratio (1:1) in volume with different etching time used: (a) 10min , b) 30min and (c) 60min.

Fig.4.2(a)-(c): Shows the AFM images of PS samples fabricated by double tank cell with (10,30,60) min. as an anodization time. The manual analysis of the AFM images profiles of samples etched at 10 and 30 minutes (figure4.2 (a-b)) could not reveal precise information about the size and type of pores that formed on the porous silicon layers of these samples. Whilst the sample etched at 60 min. (figure4.2(c) of

anodization time clearly shows three type of pores according to their diameters and depths; *meso pores* between (6-26)nm, and (0.1- 0.95)nm, respectively; *meso pores fill of meso pores* between (20-34)nm, and (0.2- 0.51)nm, respectively; *macro pores fill of meso pores* between (52-55)nm, and (0.95-1)nm, respectively.

From the obtained results we can deduce that; the longer the anodization time for double tank cell is more effective in the fabrication process of porous silicon nanostructures, which can be related to the double tank cell drawback for etching p-type Si, due to the electrolytic back side contact is biased in the reverse direction and thus does not allow substantial current flow [19] for that reason for 60 min of anodization time we could have obtained three types of pores meso pores, meso pores fill of meso pores, macro pores fill of meso pores which have a close similarity to the type of pores obtained with the designed single tank cell with difference in diameters and depths of pores in a scale of few nanometers. A good uniform backside contact with low resistance is a very important requirement for obtaining a controlled etching process; it is known that the porosity of a layer is strongly influenced by the local current density [19]. The growth of macro pore fill of meso pores type for both electrochemical cells can be realized with 60 minute of anodization time, the formations of pores increased and the pores widen further when anodization time increased [181].

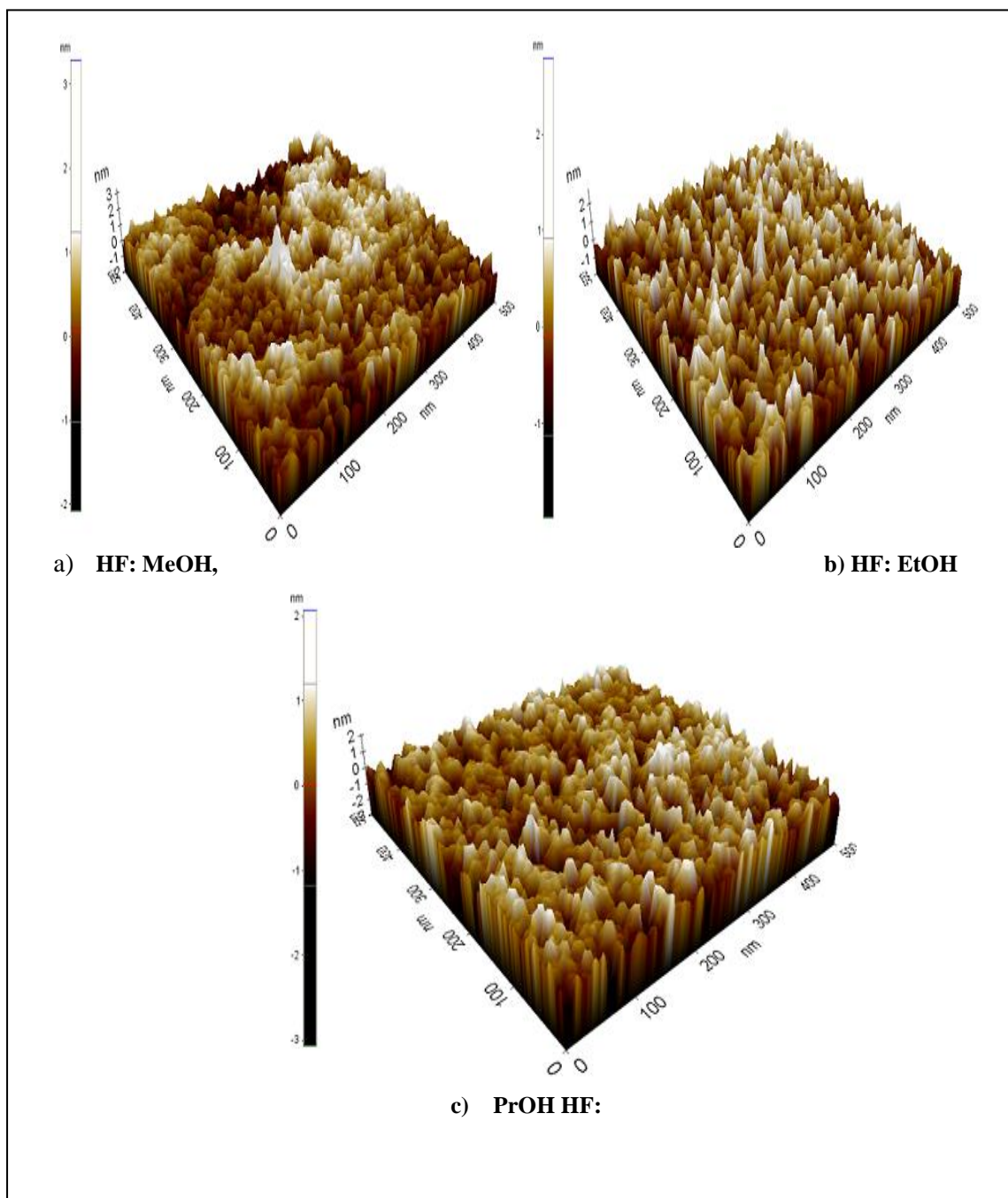


Figure 4.3 3-D AFM image of PS layer in designed single tank cell, at etching time 60 min. with different alcoholic etching solvents used : (a)HF: MeOH, (b) HF:EtOH, and (c) HF:PrOH , at ratio (1:1) in volume.

When a 3D-image of PS layer was observed with AFM, there was a difference of surface levels between the original wafer surface and the top surface of anodized part. The dissolution behavior of the top surface varies depending on the type of alcohol [182]. Fig. 4.3(a)-(c): Shows the morphology of PS layer anodized for 60 min in 48

wt.% HF solution with MeOH, EtOH and PrOH by using *designed single tank cell* . It can be found that the diameters and depths of pores when MeOH is used as solvent were: *meso pores* between (9-30) nm, and (0.13-1) nm, respectively.

With EtOH , the diameters and depths of pores were: *meso pores* between (9-37)nm, and (0.3-1.25)nm, respectively; *meso pores fill of meso pores* between (24-45)nm , and (1.25-1.63)nm, respectively; and *macro pore fill of meso pores* (63)nm, and (0.9)nm, respectively. The depths of dissolved part at the top surface and porous layer depend on the type of alcohol [182]. The polarity and the surface tension of alcohol become lower with the increasing number of carbon in alcohol [182].

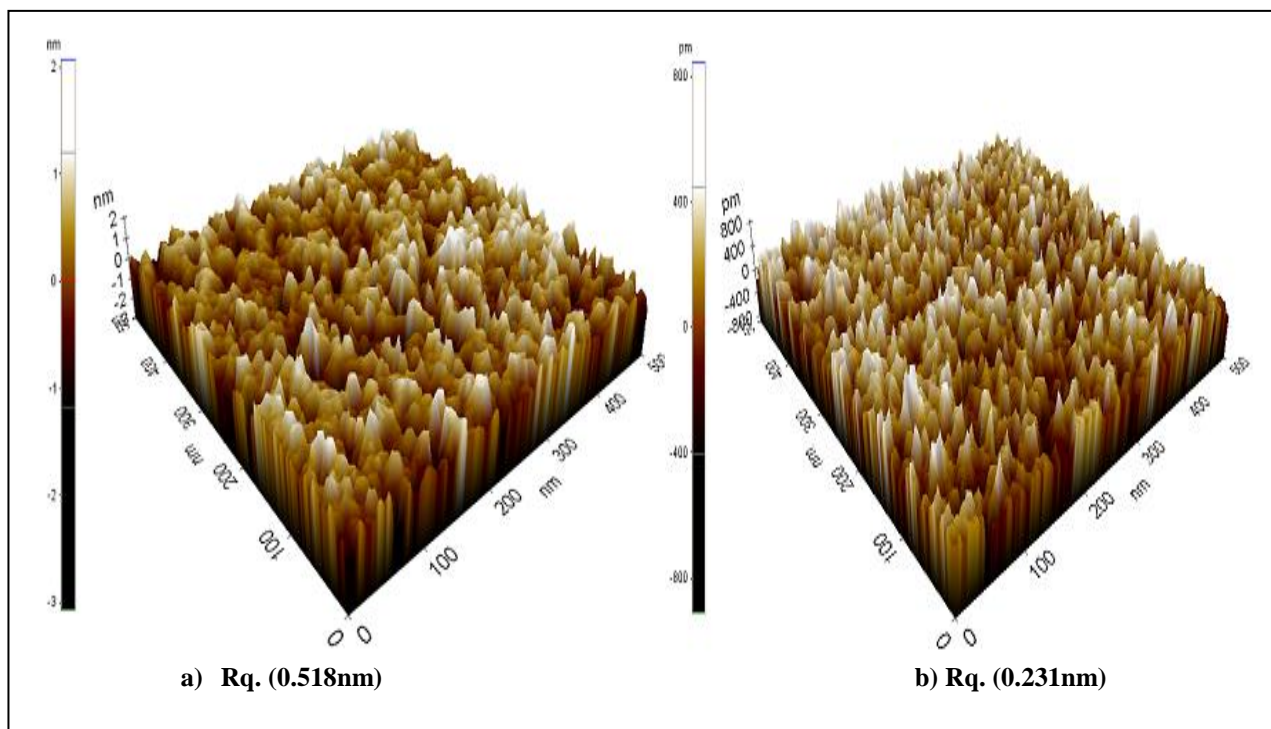


Figure 4.4 3-D AFM image of PS two layers in designed single tank cell, etched with HF: PrOH at ratio (1:1) in volume at etching time 60 min.

Surprisingly, figure 4.4(a)-(b): Shows two different layers of porous silicon PS with two different surface roughness (Rq.) (a) 0.518nm and (b) 0.231nm. When PrOH is used as solvent, the diameters and depths of pores obtained from figure 4.4(a) were: *meso pores* between (6-27)nm, and (0.13-1)nm, respectively; *meso pore fill of meso*

pores (40)nm, and (0.63)nm, respectively. While the diameters and depths of pores obtained from figure 4.4 (b) were: *meso pores* between (9-22) nm, and (0.1-0.5) nm, respectively; *meso pores fill of meso pores* (23-31) nm, and (0.2-0.51) nm, respectively. PrOH has the highest viscosity at room temperature and the lowest surface tension [183] among EtOH and MeOH. Also, PrOH is considered as a proper solvent material to help form a homogeneous-etched surface [183]. In particular, the porosity increased with decreased surface roughness and the stability of porous layers increases with the increasing carbon numbers in the alcohol at constant etched time [168,182-184].

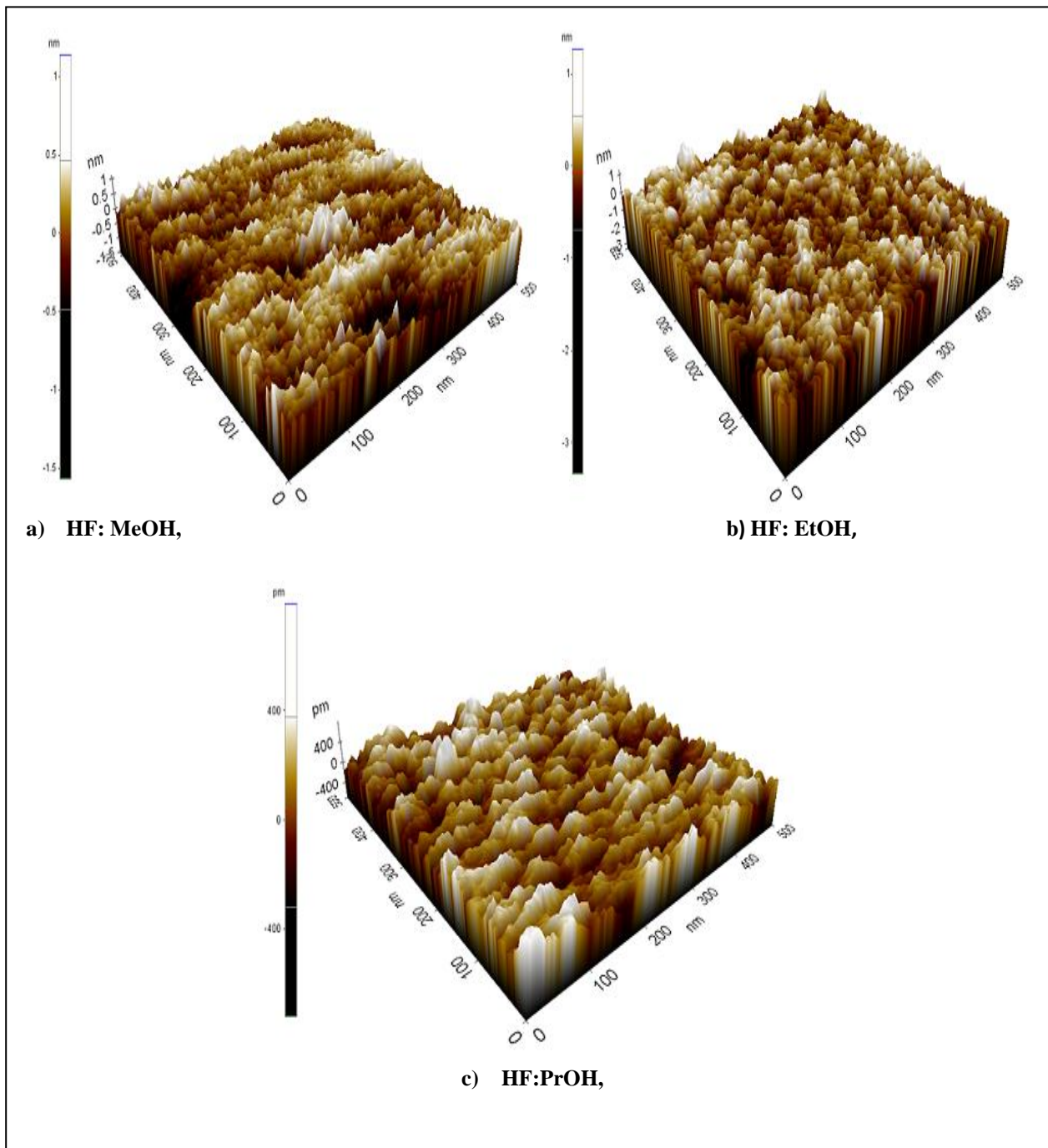


Figure 4.5 3-D AFM image of PS layer in double tank cell, at etching time 60 min. with different alcoholic etching solvents used: (a)HF:MeOH, (b) HF:EtOH, and (c) HF:PrOH, at ratio (1:1) in volume.




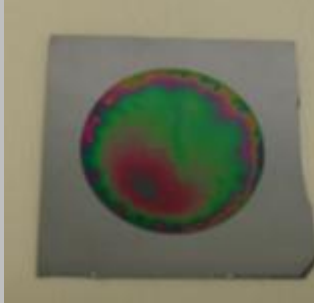


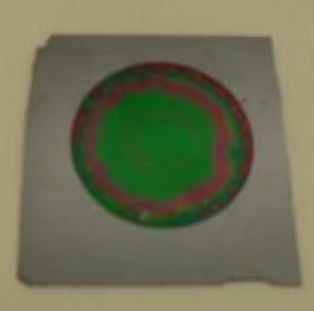

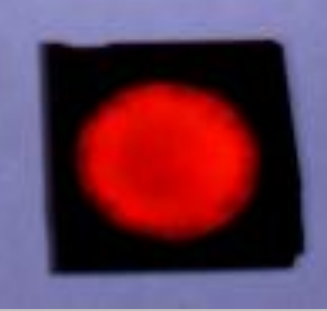
Figure 4.5(a)-(c): Shows the morphology of PS layer which anodized by using *double tank cell*. We have found that the diameters and depths of pores when MeOH is used as solvent were: *meso pores* between (7-26) nm, and (0.1-0.48) nm, respectively; *meso pores fill of meso pores* (45)nm, and (0.5)nm, respectively. With EtOH, the

diameters and depths of pores are obtained : *meso pores* between (6-26)nm, and (0.1-0.95)nm, respectively; *meso pores fill of meso pores* between (20-34)nm, and (0.2-0.51)nm, respectively; *macro pores fill of meso pores* between (52-55)nm, and (0.95-1)nm, respectively. When using PrOH, the diameters and depths of pores are obtained: *meso pores* between (6-32) nm, and (0.13-0.36)nm, respectively; *meso pore fill of meso pores* (25)nm, and (0.25)nm, respectively. In this study, figure 4.3(a)-(c), figure 4.4(a)-(b) and figure 4.5(a)-(c) provided us with a clear demonstration about the effect of the etch cell engineering, which exert a profound influence on the formation of PS layers for constant anodization time with different alcoholic solvents. For both etching cells, three main types of pores were obtained, in spite of the difference in the diameters and depths of pores were: mesopores, mesopore fill of mesopores, and macropore fill of mesopores [80], with spongy morphology were successfully produced using constant current density of $30\text{mA}/\text{cm}^2$ and constant anodization time of 60min.by varying the composition of etching solvent 48 wt.% HF solution with the following alcohols MeOH, EtOH, and PrOH at ratio (1:1) in volume. The sensitivity of pore diameter to HF concentration strongly depends on solvent [80,185]. A wider range of pore diameters can be obtained in organic solvents than in aqueous solutions [80]. Jager et al. reported an interesting fact of the degree of filling of the macro pores formed on p-Si depends on the oxidizing nature of the solution [80]: macro pores are filled with micro PS in non-oxidizing electrolyte such as acetonitrile (MeCN), while they are not filled for oxidizing electrolytes such as dimethylformamide (DMF) [80]. In other words, macro pores formed in organic solvents tend to be more filled than those formed in aqueous solutions [80]. However, Walls of the macro pores are not always covered by a micro PS layer [75,80,118,185,186].

4.2 ULTRAVIOLET PHOTOLUMINESCENCE EMISSION OF PS LAYER




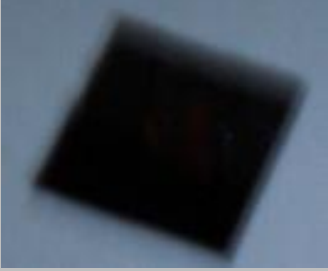


The ultraviolet (UV) photoluminescence (PL) emission from porous silicon was tested by UV lamp (254-366) nm. The influence of anodization time could be seen reflected in table 4.1 and table 4.2 which shows (UV) photoluminescence (PL) emission from porous silicon samples fabricated with two electrochemical cells with (10,30, and 60) minutes of anodization time.

Table 4.1 The images of PS samples under white light and UV (254-366) nm. with anodization electrolyte of HF: EtOH at ratio (1:1) in volume, with three anodization times, for designed single tank cell.

Time (min.)	White light	UV-254nm	UV-366nm
10			
30			
60			

Photoexcitation with blue or UV light generates confined electron–hole pairs in the nanocrystallites of porous silicon [59,187]. The energy gap of the nanocrystallites is larger than the bulk silicon bandgap (1.1 eV, corresponding to the near-infrared region of the spectrum) by the confinement energy and a visible red, orange, or green photoluminescence (PL) is observed upon recombination [59].

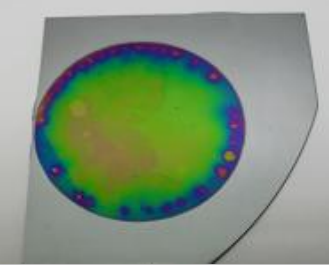
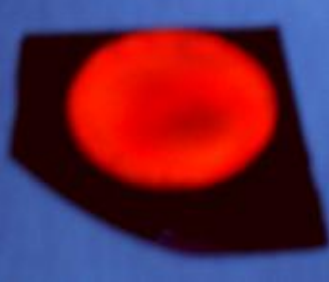
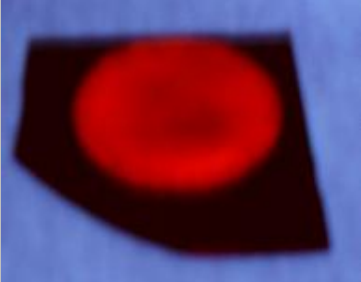
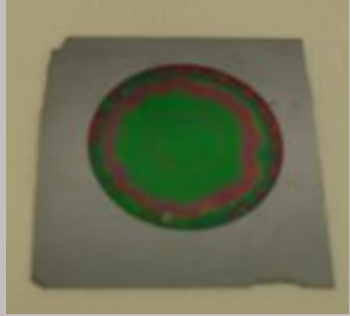
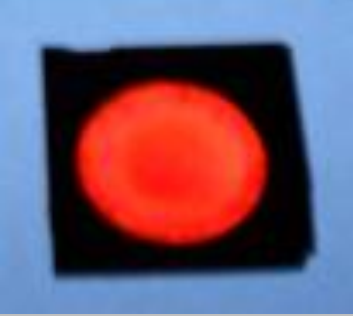

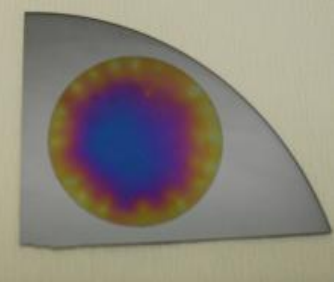


Table 4.2 The images of PS samples under white light and UV (254-366) nm. with anodization electrolyte of HF: EtOH at ratio (1:1) in volume , with three anodization times, for double tank cell.

Time	White light	UV-254nm	UV-366nm
10			none
30			none
60			none

A significant stability of UV PL emission at (254-366) nm is achieved when p-type Si is anodized in three specific alcoholic solvents used: HF: MeOH , HF:EtOH, and HF:PrOH , at ratio (1:1) in volume, etched at 60 min. by using *designed single tank cell* as shown in table 4.3. From the above results obtained by AFM and table 4.3, PS samples exhibited clear and significant stable red-orange UV PL emission increases

with increasing carbon numbers in the alcohol with slightly difference could be attributed to the diversity of type and size (diameter and depth) of pores obtained within the same cell with three specific alcoholic solvents; for MeOH were meso pores; for EtOH were meso pores, meso pores fill of meso pores and macro pore fill of meso pores; for PrOH were meso pores, meso pore fill of meso pores. The mesoporous layer exhibits a very rough texture, the mesoporous layer shows photoluminescence, whereas the macroporous layer does not [188].

Table 4.3 Shows the images of PS samples prepared by using designed single tank cell, under white light and UV (254-366) nm., with three alcoholic anodization electrolytes of: HF: MeOH, HF:EtOH, and HF:PrOH , at ratio (1:1) in volume, etched at 60 min.

	White light	UV-254nm	UV-366nm
HF: MeOH			
HF: EtOH			
HF: PrOH			

Luminescence from PS is most frequently discussed in terms of a quantum confinement model [5]. As the characteristic size of a semiconductor is reduced to the nanometer regime, confinement of the electron and hole wave functions effectively increases the band gap of the material and hence the luminescence energy [126,189]. The energy of the luminescence to increase as the feature size is decreased [121].

Table 4.4 Shows the images of PS samples prepared by using designed single tank cell and double tank cell, under white light and UV (254-366) nm., with HF:MeOH anodization electrolyte at ratio (1:1) in volume, etched at 60 min.

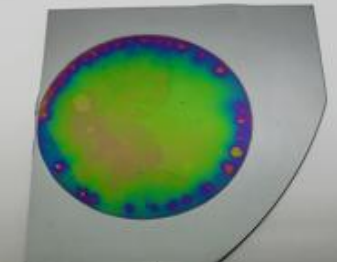
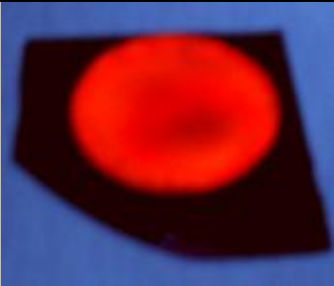
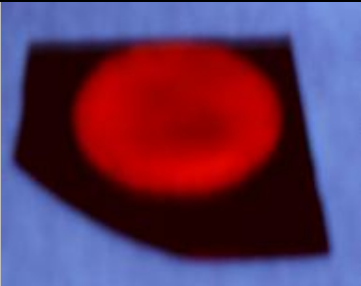



	White light	UV-254nm	UV-366nm
Single Cell			
Double Cell			

Table 4.5 Shows the images of PS samples prepared by using designed single tank cell and double tank cell, under white light and UV (254-366) nm., with HF:EtOH anodization electrolyte at ratio (1:1) in volume, etched at 60 min

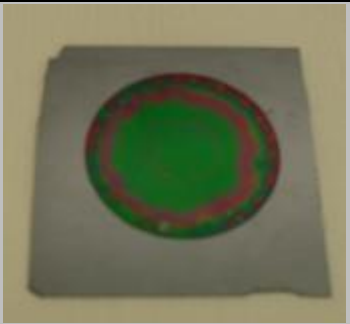




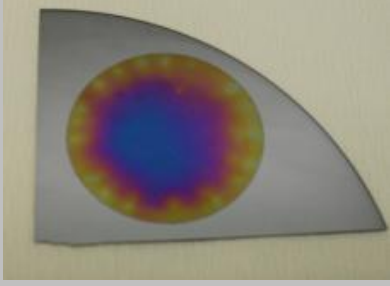




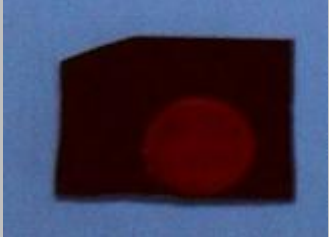
	White light	UV-254nm	UV-366nm
Single Cell			
Double Cell			none

Table 4.6 Shows the images of PS samples prepared by using designed single tank cell and double tank cell, under white light and UV (254-366) nm., with HF:PrOH anodization electrolyte at ratio (1:1) in volume, etched at 60 min.

	White light	UV-254nm	UV-366nm
Single Cell			
Double Cell			

As a comparison, the UV PL emission of porous silicon samples prepared by controlling three specific alcoholic solvents and two electrochemical cells at constant etched time are shown in tables 4.4, 4.5 and 4.6. From the above tables we can notice a clear difference in the UV PL emission, despite the fact both cells have the same type of pores for (MeOH and PrOH alcohols) but this slight difference in sizes (width and depth) in few nanometers scale and in case of EtOH alcohol, formation of macropores fill of mesopores, could be seen clearly reflected in the UV PL emission of both cells. This evident difference could be attributed to the structural factors related to the electrochemical cell design, volume of the cell (larger volume of the electrolyte is more accurate for homogeneous etching), distant of the counter electrode from the working electrode, kind of etching (vertical in case of single tank, horizontal in case of double tank), electrolyte composition (HF concentration, alcohol concentration), current density and anodization time [19,83,89,167,169,190].

4.3 I–V CHARACTERISTIC

The electrical property of the fabricated porous silicon samples were detected by I-V measurements, figure 4.6 represents the I-V characteristic of porous silicon samples with three anodization times with two electrochemical cells. The behavior of porous silicon samples show pore formation in three anodization time (10,30, and 60) minutes porous silicon forms at the exponential regions but not at potential higher than the current peak [80] .

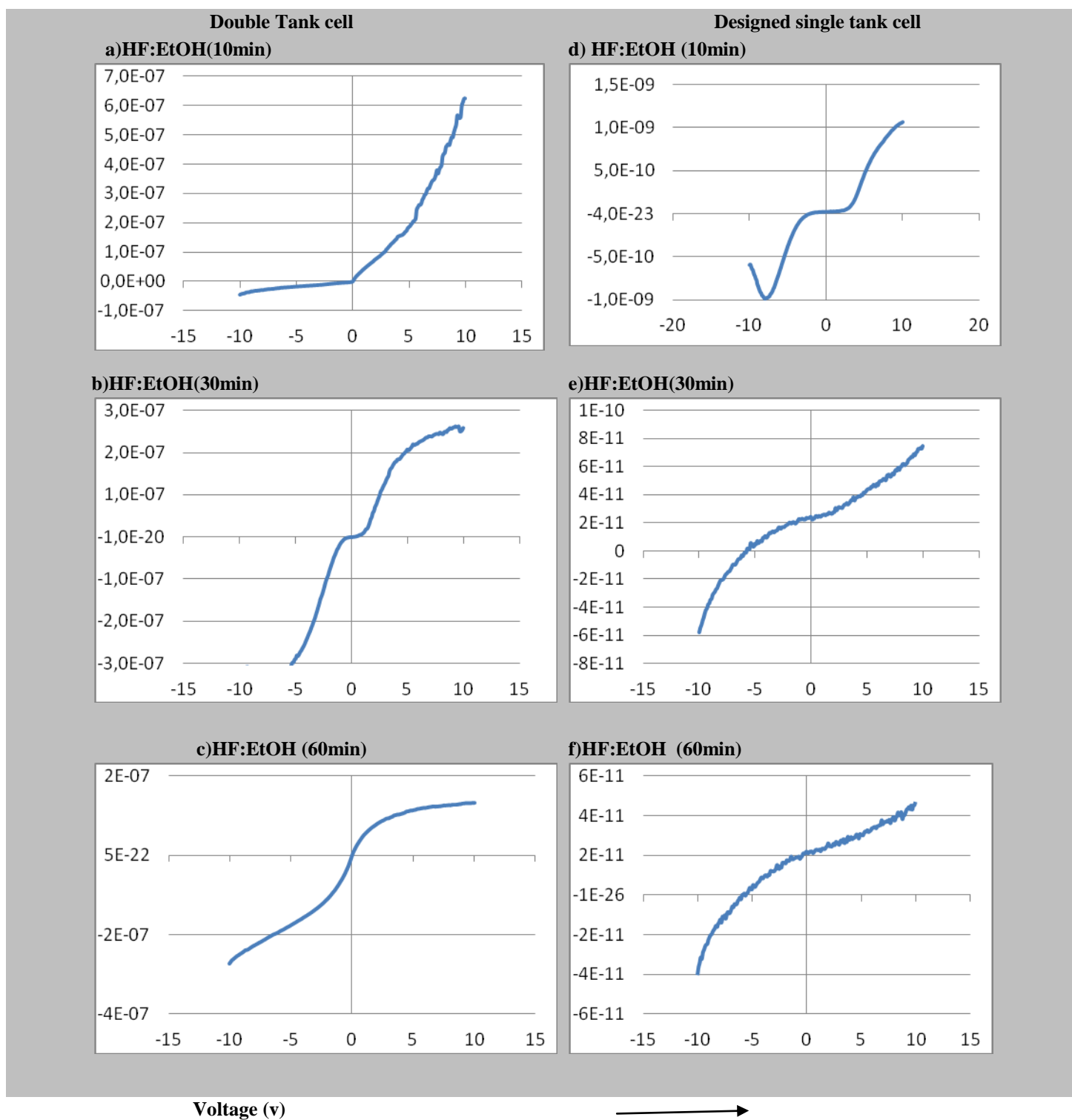


Figure 4.6 I-V measurement performed on prepared PS samples by using double tank cell (a)-(c), and designed single tank cell (d)-(f), with different etched time and constant current density $30\text{mA}/\text{cm}^2$.

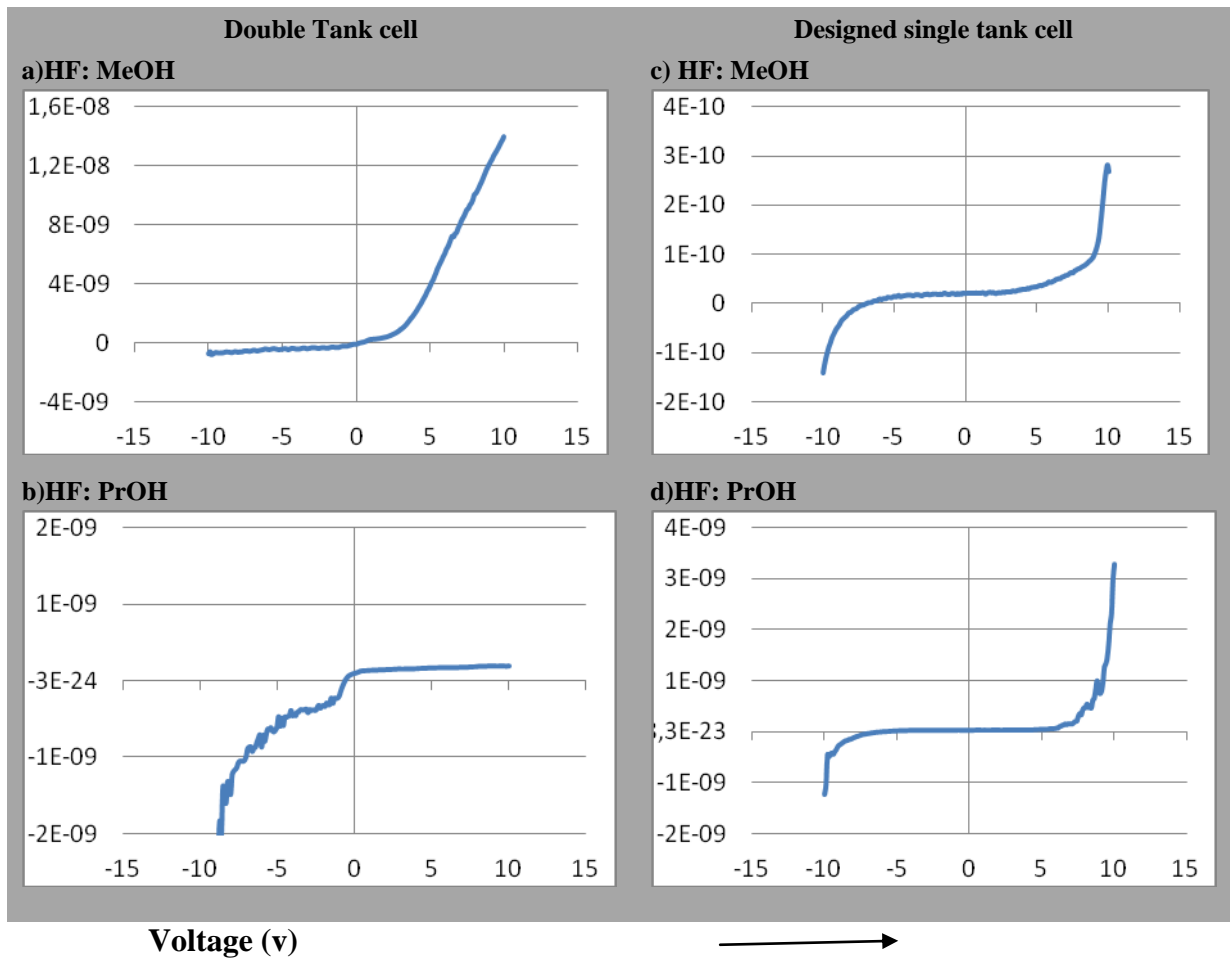


Figure 4.7 I-V measurement performed on prepared PS samples by using double tank cell (a)-(b), and designed single tank cell (c)-(d), with two different alcoholic solvents at current density $30\text{mA}/\text{cm}^2$ and etched time 60 mint

Figure 4.7(a) the I-V curve of PS sample prepared by using *double tank cell* with HF:MeOH solution shows good agreement to the experimental I-V response of the characteristics of the previous reports [191,192]. Whilst, Figure 4.7(b) the I-V curve of PS sample prepared with HF:PrOH solution shows different behavior in which we could notice, as the potential is increased; the current exhibits a peak and then remains at a relatively constant value[80].

Figure4.7(c) and (d) show the I-V curves of PS samples prepared by using *designed single tank cell* with HF:MeOH and HF:PrOH. Their behavior show basic similarity to the normal Schottky diode behavior expected from a semiconductor/electrolyte interface, but there are some important differences [3, 67].

Electropolishing region does not occur in anhydrous organic solutions due to the lack of water which is required for the formation of oxide film [80].

Accordingly, it is believed that the design of the electrochemical cell has a significant effect on the pore formation. Not only current density or concentration of HF solution but also the type of alcohol and the etch cell engineering affects the morphologies, I-V characteristics and the UV PL emission.

CHAPTER 5

CONCLUSION

A successful functionality and design of single tank cell has been proved and compared with double tank cell based on the effect of the anodization parameters. To the best of our knowledge and according to recent literatures there has not been any research that highlight the functional difference between the two designs in the matter of anodization parameters effect on the fabrication process of porous silicon nanostructures. For both etching cells, three main types of pores were obtained, in spite of the difference in the diameters and depths of pores were: mesopores, mesopore fill of mesopores, and macropore fill of mesopores. PS samples exhibited strong and stable red-orange UV PL emission without further post fabrication process treatment. The current–voltage (I-V) measurement showed basic similarities to the normal Schottky diode behavior. These two original latter properties would pave the way for porous silicon nanostructures applications in the Light emitting diodes, solar cells, sensory technology, though further investigation is required for optimization purpose

REFERENCES

- [1] Lee, M. K. and Peng, K. R., “Blue Emission of Porous Silicon”, *Applied Physics Letters*, Vol.62, pp.3159-3160, 1995.
- [2] Feng, Z.C., Yu, J.W., Li, K., Feng, Y.P., Padmanabhan, K.R. and Yang, T.R., “Combined optical, surface and nuclear microscopic assessment of porous silicon formed in HF-acetonitrile”, *Surface and Coatings Technology*, Vol. 200, pp. 3254 – 3260, 2006.
- [3] Bisi, O., Ossicini, S. and Pavesi, L., “Porous silicon: a Quantum Sponge Structure for Silicon Based Optoelectronics”, *Surface Science Reports*, Vol.38, pp.1–126, 2000.
- [4] Canham, L.T., “Silicon Quantum Wire Array Fabrication by Electrochemical and Chemical Dissolution of Wafers”, *Applied Physics Letters*, Vol. 57, pp.1046-1048, 1990.
- [5] Lehmann,V. and Gosele, U., “Porous Silicon Formation: a Quantum Wire Effect”, *Applied Physics Letters*, Vol. 58,pp.856-858, 1991.
- [6] Richter, A., Steiner, P., Kozlowski, F. and lang, W., “Current-Induced Light Emission from a Porous Silicon Device”, *IEEE Electron Device Letters*, Vol.12, pp.691-692, 1991.
- [7] Dhanekar, S.and Jain, S., “Porous Silicon Biosensor: Current Status”, *Biosensors and Bioelectronics*.Vol.41, pp.41-54, 2013.

- [8] Canham, L.T., Cox, T.I., Loni, A. and Simons, A.J., “Progress Towards Silicon Optoelectronics using Porous Silicon Technology”, *Applied Surface Science*, Vol.102, pp.436-441, 1996
- [9] Parkhutik, V., “Porous Silicon-Mechanisms of Growth and Applications”, *Solid State Electronics*, Vol.43, pp.1121–1141, 1999.
- [10] Föll, H., Christophersen, M., Carstensen, J. and Hasse, G., “Formation and Application of Porous Silicon”, *Materials Science and Engineering: R: Reports*, Vol.39, pp.93–141, 2002.
- [11] Tzur-Balter, A., Shtenberg, G. and Segal, E., “Porous Silicon for Cancer Therapy: From Fundamental Research to the Clinic”, *Review Chemical Engineering* Vol. 31, pp. 193–207, 2015.
- [12] Cheng, L., Anglin, E., Cunin, F., Kim, D., Sailor, M.J., Falkenstein, I., Tammewar, A. and Freeman, W.R., “Intravitreal properties of porous silicon photonic crystals”, *British Journal of Ophthalmology*, Vol. 92, pp.705-711, 2008.
- [13] Canham, L.T., “Bioactive Silicon Structure Fabrication through Nanoetching Techniques”, *Advanced Materials*, Vol.7, pp.1033-1037, 1995.
- [14] Canham, L.T., Reeves, C.L., King, D.O., Branfield, P.J., Crabb, J.G. and Ward, M.C.L. “Bioactive Polycrystalline Silicon”, *Advanced Materials*, Vol.8, pp.850–852, 1996.
- [15] Martinez, J.O., Chiappini, C., Ziemys, A., Faust, A.M., Kojic, M., Liu, X.W., Ferrari, M. and Tasciotti, E., “Engineering Multi-stage Nanovectors for Controlled Degradation and Tunable Release Kinetics”, *Biomaterials*, Vol.34: pp.8469 – 8477, 2013.
- [16] Lysenko, V., Bidault, F., Alekseev, S., Zaitsev, V., Barbier, D., Turpin, Ch., Geobaldo, F., Rivolo, P. and Garrone, E., “Study of Porous Silicon Nanostructures as Hydrogen Reservoirs”, *Journal of Physical Chemistry B*, Vol.109, pp.19711–19718, 2005.

- [17] Galstyan, V.E., Martirosyan, Kh.S., Aroutiounian, V.M., Arakelyan, V.M., Arakelyan, A.H. and Soukiassian, P.G., “Investigations of Hydrogen Sensors made of Porous Silicon”, *Thin Solid Films*, Vol.517, pp.239–241, 2008
- [18] Gautier, G., Kouassi, S., Desplobain, S. and Ventura, L. “Macroporous Silicon Hydrogen Diffusion Layers for Micro-Fuel Cells: From Planar to 3D Structures”, *Microelectronic Engineering*, Vol.90, pp.79–82, 2012.
- [19] Korotcenkov, G. and Cho, B.K., “Silicon Porosification: State of the Art”, *Critical Reviews in Solid State and Materials Sciences*, Vol.35, pp. 153–260, 2010.
- [20] Zeitschel, A., Friedberger, A., Welser, W. and Muller, G., “Breaking the isotropy of porous silicon formation by means of current focusing” *Sensors and Actuators*. Vol.74, pp.113–117, 1999.
- [21] Splinter, A. Sturmann, J. and Benecke, W. “New Porous Silicon Formation Technology using Internal Current Generation with Galvanic Elements” *Sensors and Actuators A*, Vol.92, pp.394–399, 2001.
- [22] Shapley, J.D.L. and Barrow, D.A., “Novel patterning Method for the Electrochemical Production of Etched Silicon”, *Thin Solid Films*, Vol. 388, pp.134–137, 2001.
- [23] Vazsonyi, E., Szilagyi, E., Petrik, P., Horvath, Z.E., Lohner, T. Fried, M. and Jalsovszky, G., “Porous Silicon Formation by Stain Etching”, *Thin Solid Films*, Vol. 388, pp.295–302, 2001.
- [24] Kolasinski, K.W., “Silicon Nanostructures from Electroless Electrochemical Etching”, *Current Opinion in Solid State and Materials Science*, Vol.9, pp.73–83, 2005.
- [25] Litvinenko, S., Alekseev, S., Lysenko, V., Venturello, A., Geobaldo, F., Gulina, L., Kuznetsov, G., Tolstoy, V., Skryshevsky, V., Garrone, E. and Barbier, D., “Hydrogen Production from Nanoporous Si Powder Formed by Stain Etching”, *International Journal of Hydrogen Energy*, Vol.35, pp.6773–6778, (2010)

- [26] Saadoun, M. , Mliki, N., Kaabi, H., Daoudi, K., Bessais, B., Ezzaouia, H. and Bennaceur, R., “Vapour-Etching-Based Porous Silicon: a New Approach”, *Thin Solid Films*, Vol. 405, pp. 29-34, 2002.
- [27] Cardinaud, C., Peignon, M.C. and Tessier, P.Y. “Plasma etching: Principles, Mechanisms, Application to Micro – and Nanotechnologies”, *Applied Surface Science*, Vol.164, pp.72–83, 2000.
- [28] Choy, C.H. and Cheah, K.W., “Laser-Induced Etching of Silicon” *Applied Physics A*, Vol.61, pp.45–50, 1995.
- [29] Chartier, C., Bastide, S. and Levy-Clement, C., “Metal-Assisted Chemical Etching of Silicon in HF-H₂O₂”, *Electrochimica Acta*, Vol.53, pp.5509–5516, 2008.
- [30] Peng, K., Hu, J., Yan, Y., Wu, Y., Fang, H., Xu, Y., Lee, S.-T. and Zhu, J., “Fabrication of Single Crystalline Nanowire by Scratching a Silicon Surface with Catalytic Metal particles”, *Advanced Functional Materials*, Vol.16, pp.387–394, 2006.
- [31] Hummel, R.E. and Ludwig, M.H., “Spark-Processing — A Novel Technique to Prepare light-Emitting, Nanocrystalline Silicon”, *Journal of Luminescence*, Vol. 68, pp.69–76, 1996.
- [32] Reynaerts, D., Meeusen, W. and Van Brussel, H., “Machining of Three-Dimensional Microstructures in Silicon by Electro-Discharge Machining”, *Sensors and Actuators A*, Vol. 67, pp. 159–165, 1998.
- [33] Naderi, N. and Hashim, M.R., “A Combination of Electroless and Electrochemical Etching Methods for Enhancing the Uniformity of Porous Silicon Substrate for Light Detection Application”, *Applied Surface Science*, Vol.258 ,pp.6436–6440 , 2012.
- [34] Naderi, N. , Hashim, M.R. and Amran, T.S.T. , “Enhanced Physical Properties of Porous Silicon for Improved Hydrogen Gas Sensing”, *Superlattices and Microstructures*, Vol. 51, pp.626–634, 2012.

- [35] Badawy, W.A., El-Sherif, R.M. and Khalil, ShA. "Porous Si Layers Preparation, Characterization and Morphology", *Electrochimica Acta*, Vol.55, pp.8563–8569, 2010.
- [36] Chen, Q., Li, X.J., Huang, J.Y., Zhou, G. and Zhang, Y.H., "Preparation and Characterization of Porous Silicon Powder" *Materials Research Bulletin*, Vol.33, pp.293–297, 1998.
- [37] Nayfeh, M.H. and Mitas, L., "Silicon Nanoparticles: New photonic and electronic material at the transition between solid and molecule", in Kumar, V. (Ed.), pp. 1–78, "Nanosilicon", *Elsevier*, Amsterdam, 2007.
- [38] Serdiuk, T., Skryshevsky, V.A., Ivanov, I.I. and Lysenko, V., "Storage of Luminescent Nanoparticles in Porous Silicon: Toward a Solid State "Golden Fleece", *Materials Letters*, Vol.65, pp.2514–2517, 2011.
- [39] Tanaka, A., Saito, R., Kamikake, T., Imamura, M. and Yasuda, H. "Electronic Structures and Optical properties of Butyl-Passivated Si Nanoparticles", *Solid State Communications*, Vol.140, pp.400–403, 2006.
- [40] Lysenko, V., Onyskevych, V., Marty, O., Skryshevsky, V.A., Chevolut, Y. and Bru-Chevallier, C., "Extraction of Ultraviolet Emitting Silicon Species from Strongly Hydrogenated Nanoporous Silicon", *Applied Physics Letters*, Vol.92, pp.251910-1-251910-3, 2008
- [41] Chaieba, S., Nayfeh, M.H. and Smith, A.D., "Assemblies of Silicon Nanoparticles Roll up into Flexible Nanotubes", *Applied Physics Letters*, Vol.87, pp. 062104-1-3, 2005.
- [42] Bai, F., Li, M., Song, D., Yu, H., Jiang, B. and Li, Y., "One-step Synthesis of Lightly Doped Porous Silicon Nanowires in HF/AgNO₃/H₂O₂ Solution at Room Temperature", *Journal of Solid State Chemistry*, Vol.196, pp.596–600, 2012.
- [43] Manilov, A.I. and Skryshevsky, V.A., "Hydrogen in Porous Silicon — A Review", *Materials Science and Engineering B*, Vol.178, pp.942-955, 2013.

- [44] Cullis, A. G., Canham, L. T. and Calcott, P. D. J., “The Structural and Luminescence Properties of Porous Silicon” *Journal of Applied Physics*, Vol. 82, pp.909-965, 1997.
- [45] Uhlir, A., “Electrolytic Shaping of Silicon and Germanium”,*The Bell System Technical Journal*, Vol.35, pp. 333-347, 1956.
- [46] Turner, D.R., “Electropolishing Silicon in Hydrofluoric Acid Solutions ”, *Journal of Electrochemical Society*, Vol. 105, pp. 402 -408, 1958.
- [47] Anglin, E.J., Cheng, L. Freeman,W.R. and M. J. Sailor, “Porous Silicon in Drug Delivery Devices and Materials”, *Advanced Drug Delivery Reviews* ,Vol.60,pp.1266-1277, 2008.
- [48] Song, H., Li, Z., Chen, H. , Jiao, Z., Yu, Z., Jin, Y., Yang, Z., Gong, M. and Sun, X., “Effect of Surface Modification by Thermally Oxidization and HF Etching on UV photoluminescence Emission of Porous silicon”, *Applied Surface Science* ,Vol.254, pp.5655-5659, 2008.
- [49] Gole, J. L. and Lewis, S. E., “Porous Silicon — Sensors and Future Applications”, in Kumar, V. (Ed.), pp. 149–175, “Nanosilicon”, *Elsevier*, Amsterdam, 2007.
- [50] Fukami, K., Harraz, F.A., Yamauchi, T., Sakka, T. and Ogata, Y.H. “Fine-Tuning in Size and Surface Morphology of Rod-Shaped Polypyrrole using Porous Silicon as Template”, *Electrochemistry Communications*, Vol.10, pp.56-60, 2008.
- [51] Ogata, Y.H., Koyama, A., Harraz, F.A., Salem, M.S. and Sakka, T., “Electrochemical Formation of Porous Silicon with Medium-Sized Pores”, *Electrochemistry*, Vol.75, pp.270-272, 2007.
- [52] Harraz, F.A., Salim, M.S., Sakka, T. and Ogata, Y.H., “Hybrid Nanostructure of Polypyrrole and Porous Silicon Prepared by Galvanostatic Technique”, *Electrochimica Acta*, Vol.53, pp.3734-3740, 2008.
- [53] Harraz, F.A., “Porous Silicon Chemical Sensors and Biosensors: A review”,

Sensors and Actuators B: Chemical, Vol.202, pp.897-912, 2014.

- [54] Gelloz, B. and Koshida, N., "Electroluminescence with High and Stable Quantum Efficiency and Low Threshold Voltage from Anodically Oxidized Thin Porous Silicon Diode", *Journal of Applied Physics*, Vol.88, pp.4319-4324, 2000.
- [55] Kim, D.-A., Shim, J.-H. and Cho, N.-H. , "PL and EL Features of P-Type Porous Silicon Prepared by Electrochemical Anodic Etching", *Applied Surface Science*, Vol.234, pp.256-261, 2004.
- [56] Langner, A., Müller, F. and Gösele, U., "Macroporous Silicon", in Hayden, O., Nielsch, K. (Eds.), *Molecular- and Nano-Tubes*, pp.431-460, Springer, New York Dordrecht Heidelberg London, 2011
- [57] Canham, L. T., Leong, W. Y., Beale, M. I. J., Cox, T. I. and Taylor, L., "Efficient Visible Electroluminescence from Highly Porous Silicon under Cathodic Bias", *Applied Physics Letters*, Vol.61, pp.2563-2565, 1992.
- [58] Ogata, Y.H., Sasano, J., Jorne, J., Tsuboi, T. Harraz, F.A., and Sakka, T., "Immersion Plating of Copper on Porous Silicon in Various Solutions", *Physica Status Solidi A-Applied Research*, Vol.182 ,pp.71-77, 2000.
- [59] Sailor, M.J., *Porous Silicon in Practice: Preparation, Characterization and Application*, first ed., Wiley-VCH Verlag GmbH & Co. KGaA, Weinheim, 2012.
- [60] Ghosh, S., Kim, H., Hong, K. and Lee, C., "Microstructure of indium tin oxide films deposited on porous silicon by rf-sputtering", *Materials Science and Engineering B*, Vol.95 pp.171-/179, 2002.
- [61] Dorvee, J. R., Sailor, M.J. and Miskelly, G. M., "Digital Microfluidics and Delivery of Molecular Payloads with Magnetic Porous Silicon Chaperones" , *Dalton Transactions* , Vol. 6, pp. 721-730, 2008.
- [62] Harraz, F.A., Sakka, T., and Ogata, Y.H., "A Comparative Electrochemical Study of Iron Deposition onto N- and P-type Porous Silicon Prepared from Lightly Doped Substrates", *Electrochimica Acta*, Vol.50, pp. 5340-5348, 2005.

- [63] Zhang, X.G. “Morphology and Formation Mechanisms of Porous Silicon”, *Journal of Electrochemical Society*, Vol. 151, pp.C69-C80, 2004.
- [64] Lehmann, V. and Gosele, U., “Porous silicon: Quantum Sponge Structures Grown via a Self-Adjusting Etching Process”, *Advanced Materials*, Vol.4, pp.114-116, 1992.
- [65] Albu-Yaron, A., Bastide, S., Maurice, J. L. and Levy-Clement, C., “Morphology of Porous N-type Silicon Obtained by Photoelectrochemical etching II: Study of The Tangled Si wires in the Nanoporous layer”, *Journal of Luminescence*, Vol.57, pp.67-71, 1993.
- [66] Rouquerol, J., Avnir, D. , Fairbridge, C.W., Everett, D.H., Haynes, J.M. , Pernicone, N., Ramsay, J.D.F., Sing, K.S.W. and Unger, K.K. , “Recommendations for The Characterization of Porous Solids”, *Pure and Applied Chemistry*, Vol.66, pp.1739–1758, 1994.
- [67] Smith, R. L. and Collins, S. D., “Porous silicon formation mechanisms”, *Journal of Applied Physics*, Vol. 71, pp.R1-R21, 1992.
- [68] Legg, K. D., Ellis, A.B. , Bolts, J.M. , and Wrighton, M. S., “N-Type Si-Based Photoelectrochemical Cell: New Liquid Junction Photocell using a Nonaqueous Ferricenium/Ferrocene Electrolyte” ,*Proceedings of the National Academy of Sciences of the United States of America*, Vol.74 , pp. 4116-41120, 1977.
- [69] Lehmann, V., Stengl, R., and Luigart, A., “On the Morphology and the Electrochemical Formation Mechanism of Mesoporous Silicon”, *Materials Science and Engineering*, Vol.B69, pp.11-22, 2000.
- [70] Lehmann, V., Luigart, A. and Corbel, V., “On the Morphology and the Electrochemical Formation Mechanism of Mesoporous Silicon”, *Electrochemical Society*, Vol.97-7, pp.132-139, 1997.
- [71] Zhang, X.G., “Mechanism of Pore Formation on N- Type Silicon”, *Journal of Electrochemical Society*, Vol.138, pp. 3750-3756, 1991.

- [72] Watanabe, Y., Arita, Y., Yokoyama, T. and Lgarashi, Y., "Formation and Properties of Porous Silicon and Its Application", *Journal of the Electrochemical Society*, Vol.122, p.1351-1355, 1975.
- [73] Levy-Clement, C., Lagoubi, A. and Tomkiewicz, M. J., "Morphology of Porous N-Type Silicon Obtained by Photoelectrochemical Etching:I. Correlations with materials and Etching parameters", *Journal of the Electrochemical Society*, Vol.141, p. 958-967, 1994.
- [74] Chazalviel, J.-N. , Wehrspohn, R. B. and Ozanam, F., "Electrochemical Preparation of Porous Semiconductors: From Phenomenology to Understanding", *Materials Science and Engineering: B* , Vol. 69-70, pp.1-10, 2000.
- [75] Lehmann, V. and Ronnebeck, S., "The Physics of Macropore Formation in Low-Doped p-Type Silicon", *Journal of the Electrochemical Society*, Vol.146, pp.2968-2975, 1999.
- [76] Hasse, G., Christophersen, M., Carstensen, J. and Föll, H. "New Insights into Si Electrochemistry and Pore Growth by Transient Measurements and Impedance Spectroscopy", *Physica Status solidi*, Vol.182, p.23-29, 2000.
- [77] Jager, C., Finkenberger, B. , Jager, W., Christophersen, M., Carstensen, J. and Föll, H., "Transmission Electron Microscopy Investigations of the Formation of Macropores in N- and P-Si (001)/ (111)," *Materials Science and Engineering* , Vol. B 69-70, pp.199-204 2000.
- [78] Ponomarev, E. A. and Levy-Clement, C., "Macropore Formation on P-type Si in Fluoride containing Organic Electrolytes" *Electrochemical and Solid-State Letters*, Vol.1, pp. 42-45, 1998.
- [79] Searson, P. C., Macaulay, J. M., and Ross, F. M., "Pore morphology and the mechanism of pore formation in n- type silicon", *Journal of Applied Physics*, Vol. 72, pp.253-258, 1992.

- [80] Zhang, G. X., "Porous Silicon: Morphology and Formation Mechanisms", in Vayenas, C., White, R. E., Gamboa-Adelco, M. E. (Eds.), *Modern Aspects of Electrochemistry*, pp.65-133, Springer, New York, 2005.
- [81] Arita, Y. and Sunohara, Y., Formation and Properties of Porous Silicon Film, *Journal of Electrochemical Society*, Vol.124, pp.285-295, 1977.
- [82] Unagami, T., "Formation Mechanism of Porous Silicon Layer by Anodization in HF Solution", *Journal of Electrochemical Society*, Vol.127, pp. 476-480,1980.
- [83] Lehmann, V. and Föll, H., "Formation Mechanism and Properties of Electrochemically Etched Trenches in N-type Silicon", *Journal of Electrochemical Society*, Vol. 137, pp. 653-659, 1990.
- [84] Al Rifai, M. H., Christophersen, M., Ottow, S., Carstensen, J. and Föll, H., "Dependence of Macropore Formation in N-Si on Potential, Temperature, and Doping", *Journal of Electrochemical Society*, Vol.147, pp.627-635, 2000.
- [85] Lehmann, V., The Physics of Macropore Formation in Low Doped N- Type Silicon, *Journal of Electrochemical Society*, Vol.140, p. 2836-2843, 1993.
- [86] Zhang, X. G., Collins, S. D. and Smith, R. L. "Porous Silicon Formation and Electropolishing of Silicon by Anodic Polarization in HF Solution", *Journal of Electrochemical Society*, Vol.136 1561-1565, 1989.
- [87] Christophersen, M., Carstensen, J. and Föll, H., "Macropore-formation on highly doped n-type silicon", *Physica Status Solidi*, (a), Vol.182, pp.45-57, 2000.
- [88] Gui, C., Elwenspoek, M., Gardeniers, J. G. E. and Lambeck, P. V. "Present and Future Role of Chemical Mechanical Polishing in Wafer Bonding", *Journal of Electrochemical Society*, Vol. 145, pp.2198 – 2204, 1998.
- [89] Lehmann, V. and Gruning, U., "The limits of macropore array fabrication", *Thin Solid Films*, Vol.297 ,pp.13-17, 1997.

- [90] Sailor, M.J., "Color Me Sensitive: Amplification and Discrimination in Photonic Silicon Nanostructures", *American Chemical Society Nano*, Vol.1, pp.248-252, 2007.
- [91] Barla, K., Bomchil, G., Herino, R., Pfister, J. C. and Baruchel J., "X-ray topographic characterization of porous silicon layers", *Journal of Crystal Growth*, Vol.68, pp.721-726, 1984.
- [92] Meiling, Y., Lu, T. and Qingnian, W., "The Influence of Preparation Conditions on the Photoluminescence of Porous Silicon Material", *Symposium on Photonics and Optoelectronics*, Shanghai, 21-23 May 2012, pp.1-3, IEEE ,2012.
- [93] Astuti, B., Rusli, N.I., Hashim, A.M., Othaman, Z., Nafarizal, N., Ali, N.K. and Safri, N.M. "Morphological and Optical Characteristics of Porous Silicon Structure Formed by Electrochemical Etching", *International Conference on Enabling Science and Nanotechnology (ESciNano)*, Kuala Lumpur , 1-3 December 2010 ,pp.1-3, IEEE,2010.
- [94] Hajji, M., Khardani ,M., Khedher N., Rahmouni, H., BessaIs, B., Ezzaouia, H. and Bouchriha, H. "Structural, Optical and Electrical Properties of Quasi-Monocrystalline Silicon Thin Films Obtained by Rapid Thermal Annealing of Porous Silicon Layers", *Thin Solid Films*, Vol. 511–512, pp. 233- 237, 2006.
- [95] Setzu, S., Lerondel, G. and Romestain, R., "Temperature Effect on the Roughness of the Formation Interface of P-Type Porous Silicon", *Journal of applied physics*, Vol.84, pp.3129-3133, 1998
- [96] Herino R., "Pore size distribution in porous silicon", in Canham, L.T., (Ed.), *Properties of porous silicon*, The Institution of Electrical Engineers, Chapter 2.2, London, 1997.
- [97] Bomchil, G., Herino, R., Barla, K. and Pfister, J. C. , "Pore Size Distribution in Porous Silicon Studied by Adsorption Isotherms," *Journal of the Electrochemical Society*, Vol.130, pp.1611-1614, 1983.

- [98] Herino, R., Bomchil, G., Barla, K., Bertrand, C. and Ginoux, J. L., "Porosity and Pore Size Distributions of Porous Silicon Layers", *Journal of the Electrochemical Society*, Vol.134, pp.1994-2000, 1987.
- [99] Jarvis, K. L., Barnes, T. J. and Prestidge, C. A. "Surface chemistry of porous silicon and implications for drug encapsulation and delivery applications", *Advances in Colloid and Interface Science*, Vol.175, pp.25-38, 2012.
- [100] Diaz, D. C., Osmanski, M., Guan, H. and Das, B., "An Improved Fabrication Technique for Porous Silicon", *Review of Scientific Instruments*, Vol.64, pp.507-509, 1993.
- [101] Grigoras, K. and Pacebutas, V., "Porous Silicon Fabrication Technique for Large Area Devices", *Review of Scientific Instruments*, Vol.67, pp.2337-2338, 1996.
- [102] Halimaoui, A. "Porous silicon: material processing, properties and applications" in Vial, J.-C and Derrien, J. (Eds.), *Porous Silicon Science and Technology*, pp.33-52, Springer, Berlin, 1995.
- [103] Osorio-Saucedo, R., Vazquez-Lopez, C., Calleja, W., Allred, D.D. and Falcony, C., "A Rotating Electrochemical Cell to Prepare Porous Silicon with Different Surface Structures", *Thin solid Films*, Vol. 338, pp. 100-104, 1999.
- [104] Halimaoui, A., "A Porous Silicon Formation: Anodisation Cells" In: Canham, L.T., (Ed), *Properties of porous silicon*, The institution of Electrical Engineers, Chapter 1.2, London, 1997.
- [105] Lang, W., Steiner, P. and Sandmaier, H., "Porous silicon: A Novel Material for Microsystems", *Sensors and Actuators A*, Vol.51, pp.31-36, 1995. [106] Xu, H., Xiao, H., Pei, H., Cui, J. and Hu, W., "Photodegradation Activity and Stability of Porous Silicon Wafers with (1 0 0) and (1 1 1) Oriented Crystal Planes", *Microporous and Mesoporous Materials*, Vol.204, pp.251-256, 2015.
- [107] Lai, C., Li, X., Liu, C., Guo, X., Xiang, Z., Xie, B. Zou, L., "Improvement in Gravimetric Measurement for Determining the Porosity and Thickness of

- Porous Silicon using an Optimized Solution”, *Materials Science in Semiconductor Processing*, Vol.26, pp.501-505, 2014.
- [108] Harraz, F.A., Salem, A.M., Mohamed, B.A., Kandil, A. and Ibrahim, I.A., “Electrochemically Deposited Cobalt/Platinum (Co/Pt) Film into Porous Silicon: Structural Investigation and Magnetic Properties”, *Applied Surface Science*, Vol.264, pp.391-398, 2013.
- [109] Steiner, P., Kozlowski, F. and Lang, W., “Blue and green electroluminescence from a porous silicon device” , *IEEE Electron Device Letters* ,Vol. 14, pp.317-319, 1993.
- [110] Lang, W., Richter, A., Steiner, P., Kozlowski, F., Sandmaier, H. and Ruge, I., “Current induced light emission from nanocrystalline silicon structures”, *Micro Electro Mechanical Systems, 1992, MEMS '92, Proceedings. An Investigation of Micro Structures, Sensors, Actuators, Machines and Robot* , Travemunde, Germany, 4-7 February 1992, pp.99-103,IEEE.
- [111] Shih, S., Tsai, C., Li, K.-H. , Jung, H.H. , Campbell J.C. and Kwong, D.L. , “Control of porous Si photoluminescence through dry oxidation”, *Applied Physics Letters*, Vol. 60, pp. 633-635 ,1992.
- [112] Li, S., Ma, W., Zhou, Y., X. Chen, Ma, M., Xiao, Y. and Xu, Y. “Influence of Fabrication Parameter on the Nanostructure and Photoluminescence of Highly Doped P-Porous Silicon”, *Journal of Luminescence*, Vol.146, pp.76-82, 2014.
- [113] Jian-Ming, J., Xiu-Xia, H., Qian, D .and Zhen-Xin, W., “Preparation of Porous Silicon Substrate for Protein Microarray Fabrication by Double-Cell Electrochemical Etching Method”, *Chinese Journal of Analytical Chemistry*, Vol.41, pp.698-703, 2013.
- [114] Riley, D.W. and Gerhardt, R.A., “Effect of porosity on the optical properties of anodized porous silicon thin films”, *Conference on Electrical Insulation and Dielectric Phenomena, 1998, Annual Report, Atlanta, Georgia, 25-28 October 1998, Vol.1, pp. 248 –251, IEEE, Georgia,1998.*

- [115] Suhaimi, M.H.F., Zubaidah, M. A., Yusop, S.F.M., Rusop, M. and Abdullah, S., "The effect of surface morphology to photoluminescence spectrum porous silicon", Conference on Semiconductor Electronics (ICSE), 2012 10th IEEE International, Kuala Lumpur, 19-21 September 2012, pp.149-152, IEEE,2012.
- [116] Milani, SH. D., Dariani, R. S., Mortezaali, A., Daadmehr, V. and Robbie, K., "The correlation of morphology and surface resistance in porous silicon", Journal of Optoelectronics and Advanced Materials, Vol.8, pp.1216-1220, 2006.
- [117] Salman, K. A., Omar, K., and Hassan, Z., "Effect of etching time on porous silicon processing", International Conference on Nanotechnology - Research and Commercialization 2011, Sabah Malaysia, 6-9 June 2011, Vol.1502, pp. 280-287, 2011
- [118] Christophersen, M., Carstensen, J., Feuerhake, A. and Föll, H., "Crystal orientation and electrolyte dependence for macropore nucleation and stable growth on p-type-silicon", Materials Science and Engineering, B69-70, pp.194-198, 2000.
- [119] Hirschman, K. D., "Light Emission from Nanoscale Silicon: The king of Microelectronics Advancing toward Optoelectronic Integrated Circuits", University/Government/Industry Microelectronics Symposium, 1997, Proceedings of the Twelfth Biennial, Rochester, NY, 20-23 Jul 1997, pp.177-182, 1997.
- [120] Stutzmann, M. Brandt, M.S., Rosenbauer, M. Weber, J., and Fuchs, H.D, "Photoluminescence Excitation Spectroscopy of Porous Silicon and Siloxene", Physical Review B, Vol.47, pp.4806-4809, 1993.
- [121] Read, A.J., Needs, R. J., Nash, K.J., Canham, L.T. , Calcott, P.D.J. and Qteish, A., "First-principles calculations of the electronic properties of silicon quantum wires", Physical Review Letters, Vol.69, pp.1232-1235, 1992.
- [122] Hybertsen, M.S., "Mechanism for Light Emission from Nanoscale Silicon", in Vial, J.C., Derrien, J. (Ed.), Porous Silicon Science and Technology, pp.67-90, Springer, Berlin Heidelberg 1995.

- [123] Koch, F., Petrova-Koch, V., Muschik, T., Nikolov, A. and Gavrilenko, V., "Some Perspectives on the Luminescence Mechanism via Surface-Confined States of Porous Si" ,Materials Research Society Symposium Proceedings on Microcrystalline Semiconductors–Materials Science and Devices, Germany, Vol. 283, pp.197-202, 1993.
- [124] Prokes, S.M. and Gletnbocki, O.J. "Role of interfacial oxide-related defects in the red-light emission in porous silicon", Phys. Rev. B, Vol.49, pp.2238-2241, 1994.
- [125] Li, K.-H. , Tsai, C., Sarathy, J. and Campbell, J.C., "Chemically induced shifts in the photoluminescence spectra of porous silicon", Applied Physics Letters, Vol.62, pp. 3192-3194, 1993.
- [126] Collins, R.T., and Tischler, M. A., "Porous Silicon Sheds a New Light on OEICs" Circuits and Devices Magazine, IEEE, Vol.9, pp.23-28, 1993.
- [127] Mizuno, H., Koyama, H. and Koshida, N., "Oxide- Free Blue Photoluminescence from Photochemically Etched Porous Silicon", Applied Physics Letters, Vol.69, pp.3779, 1996.
- [128] Harvey, J. F., Shen, H., Lux, R. A., Dutita, M., Pamulapati, J. and Tsu, R., "Raman and Optical Characterization of Porous Silicon", Materials Research Society Symposium Proceedings on Light emission from silicon, Vol.256, pp.175-178, 1992.
- [129] Kovalev, D. I., Yarostietzkii, I. D. , Muschik, T., Petrova-Koch, V. and Koch, F., "Fast and Slow Visible Luminescence Bands of Oxidized Porous Si" ,Applied Physics Letters, Vol. 64, pp.214-216, 1994.
- [130] Canham, L. T., "Luminescence Bands and their Proposed Origins In Highly Porous Silicon", Physica Status Solidi, B, Vol.190, pp.9-14, 1995.
- [131] Tsybeskov, L., Vandyshv, Ju. V. and Fauchet, P. M., "Blue Emission in Porous Silicon: Oxygen-Related Photoluminescence", Physical Review B, Vol. 49, pp.7821-7824, 1994.

- [132] Harris, C. I., Syvajarvi, M., Bergman, J. P., Kordina, O., Henry, A., Monemar, B. and Janzen, E., "Time- Resolved Decay of the Blue Emission in Porous Silicon", *Applied Physics Letters*, Vol.65, pp.2451-2453, 1994.
- [133] Kux, A., Kovalev, D. and Koch, F., "Time- Delayed Luminescence from Oxidized Porous Silicon After Ultraviolet Excitation", *Applied Physics Letters*, Vol.66, pp. 49-51, 1995.
- [134] Kux, A., Kovalev, D. and Koch, F., "Slow Luminescence from Trapped Charges in Oxidized Porous Silicon", *Thin Solid Films*, Vol.255, pp.143 -145, 1995.
- [135] Fauchet, P. M., Ettedgui, E., Raisanen, A., Brillson, L. J., Seiferth, F., K.Kurinec, S., Gao, Y., Peng, C. and Tsybeskov, L., "Can Oxidation And Other Treatments Help Us Understand The Nature Of Light-Emitting Porous Silicon?" *Materials Research Society Symposium Proceedings*, Vol.298, p.271-276, 1993.
- [136] Jiang, D. T., Coulthard, I., Sham, T. K. , Lorimer, J. W. , Frigo, S. P. , Feng, X. H. and Rosenberg, R. A. , "Observations on the surface and bulk luminescence of porous silicon", *Journal of Applied Physics*, Vol.74, pp.6335-6340 , 1993.
- [137] Zuk, J. Kuduk, R., Kulik, M., Liskiewicz, J., Maczka, D. Zhukovski, P. V. , Stelmakh, V.F., Bondarenko,V.I. and Dorofeev, A. M. , "Ionoluminescence of porous silicon" , *Journal of Luminescence* ,Vol.57, pp.57-60, 1993.
- [138] Lin, J. Yao, G. Q., Duan, J. Q. and Qin, G.G., "Ultraviolet Light Emission from Oxidized Porous Silicon", *Solid State Communications*, Vol.97, pp.221-224, 1996.
- [139] Coulthard, I., Jiang, D. T. and Sham, T. K., "VUV Induced Luminescence from Porous Silicon", *Journal of Electron Spectroscopy and Related Phenomena*, Vol.79, pp.233-236, 1996.
- [140] Qin, G. G. , Lin, J., Duane, J. Q. and Yao, G. Q., "A Comparative Study Of Ultraviolet Emission With Peak Wavelengths Around 350 nm from Oxidized Porous Silicon and that from SiO₂ Powder", *Applied Physics Letters*, Vol. 69, pp.1689-1691, 1996.

- [141] Chen, Q., Zhou, G., Zhu, J., Fan, C., Li, X. G. and Zhang, Y., "Ultraviolet light emission from porous silicon hydrothermally prepared", *Physics Letters A*, Vol. 224, pp.133-136, 1996.
- [142] Theunissen, M. J. J., "Etch Channel Formation during Anodic Dissolution of N-Type Silicon in Aqueous Hydrofluoric Acid", *Journal of the Electrochemical Society*, Vol.119, pp.351-360, 1972.
- [143] Searson, P.C., "Porous silicon membranes", *Applied Physics Letters*, Vol.59, pp.832-833, 1991.
- [144] Bsiesy, A., Vial, J.-C. , Gaspard, F., Herino, R., Ligeon, M. , Muller, F., Romestain, R., Wasiela, A., Halimaoui, A. and Bomchil, G., "Photoluminescence of High Porosity and of Electrochemically Oxidized Porous Silicon Layers", *Surface Science*, Vol. 254, pp.195-200, 1991.
- [145] Koshida, N. and Koyama, H., "Efficient Visible Photoluminescence from Porous Silicon", *Japan Journal of Applied Physics*, Vol.30, L1221-L1223, 1991.
- [146] Levy-Clement, C., Lagoubi, A., Ballutaud, D., Ozanam, F., Chazalviel, J. N. and Neumann-Spallart, M., "Porous N-silicon Produced by Photoelectrochemical Etching", *Applied Surface Science*, Vol. 65-66, pp.408-414, 1993.
- [147] Beale, M. J., Chew, N. G., Uren, M. J., Cullis, A.G. and Benjamin, J. D., "Microstructure and formation mechanism of porous silicon", *Applied Physics Letters*, Vol.46, pp.86-88, 1985.
- [148] Beale, M. I. J., Benjamin, J. D., Uren, M. J., Chew, N. G. and Cullis, A. G., "An Experimental and Theoretical Study of the Formation and Microstructure of Porous Silicon", *Journal of Crystal Growth*, Vol.73, pp.622-636, 1985.
- [149] Searson, P.C. and Zhang, X.G., "The anodic dissolution of silicon in HF solutions", *Journal of the Electrochemical Society*, Vol.137, pp. 2539-2546 , 1990.

- [150] Canham, L. T. and Groszek, A. J., "Characterization of Microporous Si by Flow Calorimetry: Comparison with a Hydrophobic SiO₂ Molecular Sieve", *Journal of Applied Physics*, Vol.72, pp.1558-1565, 1992.
- [151] Cullis, A. G., Canham, L. T., Williams, G. M., Smith, P. W. and Dosser, O.D., "Correlation of the Structural and Optical Properties of Luminescent, Highly Oxidized Porous Silicon", *Journal of Applied Physics*, Vol.75, pp.493-501, 1994.
- [152] Chuang, S-F., Collins, S. D. and Smith, R. L., "Preferential Propagation of Pores during the Formation of Porous Silicon: A Transmission Electron Microscopy Study", *Applied Physics Letters*, Vol. 55, pp.675-677, 1989.
- [153] Cullis, A. G. and Canham, L. T., "Visible Light Emission due to Quantum Size Effects in Highly Porous Crystalline Silicon", *Nature*, Vol. 353, 335 -338, 1991.
- [154] Cole, M. W., Harvey, J.F., Lux, R. A., Eckart, D. W. and Tsu, R., "Microstructure of visibly luminescent porous silicon", *Applied Physics Letters*, Vol. 60, pp.2800-2802, 1992.
- [155] Nishida, A., Nakagawa, K., Kakibayashi, H. and Shimada, T., "Microstructure of Visible Light Emitting Porous Silicon", *Japanese Journal of Applied Physics of Visible Light Emitting Porous Silicon*, *Japanese Journal of Applied Physics*, Vol. 31, L1219-L1222, 1992.
- [156] Nakajima, A., Ohshima, Y., Itakura, T. and Goto, Y., "Microstructure of Porous Silicon", *Applied Physics Letters*, Vol.62, pp.2631-2633, 1993.
- [157] Weng, Y.M., Fan, Zh. N. and Zong, X. F., "Luminescence studies on porous silicon", *Applied Physics Letters*, Vol.63, pp.168 -170, 1993.
- [158] Berbezier, I. and Halimaoui, A., "A microstructural study of porous silicon", *Journal of Applied Physics*, Vol.74, pp.5421-5425, 1993.
- [159] Kalkhoran, N.M., Namavar, F. and Maruska, H. P., "Optoelectronic applications of porous polycrystalline silicon", *Applied Physics Letters*, Vol. 63, 2661 - 2663, 1993.

- [160] Ono, H., Gomyu, H., Morisaki, H., Nozaki, S., Show, Y., Shimasaki, M., Iwase, M. and Izumi, T., "Effects of Anodization Temperature on Photoluminescence from Porous Silicon" *Journal of Electrochemical Society*, Vol.140, L180-L182, 1993.
- [161] Steiner, P. and Lang, W., "Micromachining Applications of Porous Silicon", *Thin Solid Films*, Vol. 255, pp.52-58, 1995.
- [162] Petrova-Koch, V. and Muschik, T., "The Relation between the Visible and the Infrared Luminescence Bands in Porous Silicon; Comparison with Amorphous Si Alloys", *Thin Solid Films*, Vol. 255, pp.246-249, 1995.
- [163] Delerue, C., Lannoo, M., Allan, G. and Martin, E., "Theoretical descriptions of porous silicon", *Thin Solid Films*, Vol.255, pp.27-34, 1995.
- [164] Lee, C.H., Yeh, C.C., Hwang, H.L. and Hsu, K.Y.J., "Characterization of Porous Silicon-on-Insulator Films Prepared by Anodic Oxidation", *Thin Solid Films*, Vol. 276, pp.147-150, 1996.
- [165] Berbezier, I., Martin, J.M., Bernardi, C. and Derrien, J., "EELS Investigation of Luminescent Nanoporous P-type Silicon", *Applied Surface Science*, Vol.102, pp.417-422, 1996.
- [166] Propst, E.K. and Kohl, P.A., "The Electrochemical Oxidation of Silicon and Formation of Porous Silicon in Acetonitrile", *Journal of Electrochemical Society*, Vol.141, pp.1006 -1013, 1994.
- [167] Carstensen, J., Christophersen, M. and Föll, H. "Pore Formation Mechanisms for the Si-HF System", *Materials Science and Engineering: B*, Vol.69-70, pp.23-28, 2000.
- [168] Christophersen, M., Carstensen, J., Voigt, K., and Föll, H., "Organic and Aqueous Electrolytes Used for Etching Macro - and Mesoporous Silicon", *Physics status solidi (a)*, Vol.197, pp.34 -38, 2003. [169] Jakubowicz, J., "Nanoporous Silicon Fabricated at Different Illumination and Electrochemical Conditions", *Superlattices and Microstructures*, Vol.41, pp.205-215, 2007.

- [170] Ge, D.H., Jiao, J.W., Zhang, S. and Wang, Y.L., "Fast Speed Nano-Sized Macropore Formation on Highly-Doped N-Type Silicon via Strong Oxidizers", *Electrochemistry Communications*, Vol. 12, pp.603–606, 2010.
- [171] Guerrero-Lemus, R., Moreno, J. D., and Martinez-Duart, J. M., "Electrochemical Cell for the Preparation of Porous Silicon", *Review of Scientific Instruments*, Vol.67, pp.3627-3630, 1996.
- [172] Servidori, M., Ferrero, C., Lequien, S., Milita, S., Parisini, A. Romestain, R., Sama, S., Setzu, S. and Thiaudie, D., "Influence of the Electrolyte Viscosity on the Structural Features of Porous Silicon", *Solid State Communications*, Vol.118, pp.85-90, 2001.
- [173] Setzu, S., Letant, S., Solsona, P., Romestain, R. and Vial, J.C., "Improvement of the Luminescence in P-type as-Prepared or Dye Impregnated Porous Silicon Microcavities", *Journal of Luminescence*, Vol.80, pp.129–132, 1999.
- [174] Binnig, G., Quate, C.F. and Gerber, C., "Atomic Force Microscope", *Physical Review Letters*, Vol.56, pp. 930-933, 1986.
- [175] Bruening, F. A. and Cohen, A. D., "Measuring surface properties and oxidation of coal macerals using atomic force microscope". *International Journal of Coal Geology*, Vol.63 pp.195-204, 2005
- [176] Poon, C.Y. and Bhushan, B., "Comparison of surface roughness measurements by stylus profiler, AFM and non-contact optical profiler", *Wear*, Vol.191, pp.76-88, 1995.
- [177] SuPing, Y., Kun, J., Ke, Z., WenXuan, H., Hai, D., MiaoChun, L. and WenMing, P., "An atomic force microscopy study of coal nanopore structure", *Chinese Science Bulletin*, Vol.56, pp.2706-2712, 2011.
- [178] Meyer, E., "Atomic Force Microscopy", *Progress in Surface Science*, Vol. 41, pp. 3-49, 1992.

- [179] Tsai, C., Li, K.-H., Campbell, J.C., Hance, B. K., Arendt, M. F., White, J. M., Yau, S.-L. and Bard, A. J., "Effects of Illumination during Anodization of Porous Silicon", *Journal of Electronic Materials*, Vol. 21, pp.995-1000, 1992.
- [180] Veeco Instruments Inc. Nanoscope Software 6.13 User Guide, 2002.
- [181] Zubaidah, M.A., Rusop, M., Abdullah, S., "Electroluminescence and photoluminescence properties of porous silicon nanostructures with optimum etching time of photo-electrochemical anodization", 2012 IEEE International conference on Electronics Design, Systems and Applications (ICEDSA), Kuala Lumpur, Malaysia, 5-6 Nov. 2012
- [182] Urata, T., Fukami, K., Sakka, T. and Ogata, Y. H., "Pore formation in p-type silicon in solutions containing different types of alcohol", *Nanoscale Research Letters*, Vol.7:329, pp.1-5, 2012.
- [183] Kim, H. and Cho, N., "Morphological and nanostructural features of porous silicon prepared by electrochemical etching", *Nanoscale Research Letters*, Vol. 7:408, pp.1-8, 2012.
- [184] Song, J.H., Sailor, M.J., "Dimethyl sulfoxide as a mild oxidizing agent for porous silicon and its effect on photoluminescence", *Inorganic Chemistry*, Vol.37, pp.3355-3360, 1998.
- [185] Zhang, X.G., *Electrochemistry of Silicon and Its Oxide*, Springer, New York, 2001.
- [186] Gronet, C. M., Lewis, N. S., Cogan, G. and Gibbons, J., "n-Type silicon photoelectrochemistry in methanol: Design of a 10.1% efficient semiconductor/liquid junction solar cell", *Proceedings of the National Academy of Sciences of USA*, Vol.80, pp.1152-1156, 1983.
- [187] Calcott, P.D.J., Nash, K.J., Canham, L.T., Kane, M.J., Brumhead, D., "Spectroscopic identification of the luminescence mechanism of highly porous Si", *Journal of Luminescence*, Vol.57, pp.257-269, 1993.
- [188] Williams, P., Lévy-Clement, C., P'eu, J.-E., Brun, N., Colliex, Ch.,

- Wehrspohn, R., Chazalviel, J.-N. , and Albu-Yaron, A., “Microstructure and photoluminescence of porous Si formed on n-type substrates in the dark”, *Thin Solid Films*, Vol.298 pp.66-, 1997.
- [189] Buda, F., Kohanoff , J. and Parrinello, M. , *Physical Review Letters*, “Optical properties of porous silicon: A first-principles study” ,Vol.69, pp.1272-1275, 1992.
- [190] Lehmann, V., “Developments in porous silicon research”, *Materials Letters* ,Vol.28 ,pp.245-249,1996.
- [191] Achour, Z. B. , Touayar, O. and Sifi, N., “Stability Study of the Metrological Characteristics of a ZnO/PS/C-Si Photodiode (PSiZ) Used as a Transfer Standard in the Visible Spectral Range”, *Modern Instrumentation*, Vol.1 ,pp.21-25,2012.
- [192] Atyaoui, M., Dimassi , W., Khalifa, M., Chtourou , R.and Ezzaouia, H., “Improvement of photoluminescence and electrical properties of porous silicon layer treated with lanthanum” , *Journal of Luminescence*, Vol. 132 ,pp. 2572–2576, 2012.
- [193] Ming K. Lee ; K. R. Peng ; C. H. Chu, "Porous silicon photodetector"", *Proc SPIE* 2101, *Measurement Technology and Intelligent Instruments*, 1060,September 22, 1993.
- [194] Miranda, C. R. B. , Baldan, M. R. , Beloto, A. F.and Ferreira, N. G. , “Morphological and Optical Characteristics of Porous Silicon Produced by Anodization Process in HF-Acetonitrile and HF-Ethanol Solutions”, *Journal of Brazilian Chemical Society* , Vol. 19, pp. 769-774, 2008.
- [195] Martin-Palma,R. J., Manso-Silvan, M. and Torres-Costa, V., “ Biomedical applications of nanostructured porous silicon: a review ”, Vol.4, 2010.
- [196] Freeman, W. R., Sailor, M.J. and Cheng, L ., “Materials and methods for delivering compositions to selected tissues ”, *The Regents of The University Of California patents*, Patent Application 20100196435.

- [197] Korotcenkov, G., *Porous Silicon: From Formation to Application: Formation and Properties*, CRC Press 2015, pp. 73–125.
- [198] Gösele, U. and Lehmann, V., “Light-emitting porous silicon”, Vol.40, pp. 253–259, 1995.
- [199] Campbell, J.C. , Li, K.-H. and Tsai, C., Luminescence from Si-based structures, International Electron Devices Meeting, pp.643-646, 13-16 Dec. 1992, San Francisco, CA, USA,1992.